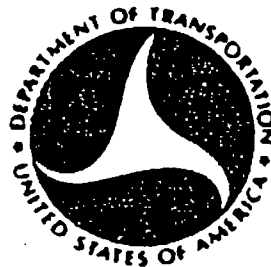


NATIONAL CRASH SEVERITY STUDY - QUALITY CONTROL

Task V: Analysis to Refine Spinout
Aspects of CRASH

Raymond R. McHenry
Brian G. McHenry

Calspan Field Services, Inc.
P.O. Box 400
Buffalo, New York 14225



January 1981
Final Report

Document is available to the public through
the National Technical Information Service,
Springfield, Virginia 22161

Prepared for
U.S. DEPARTMENT OF TRANSPORTATION
National Highway Traffic Safety Administration
Washington, D.C. 20590

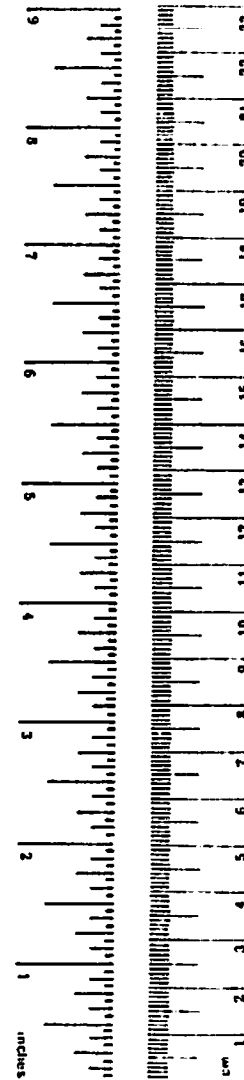
TECHNICAL REPORT STANDARD TITLE PAGE

1. Report No.		2. Government Accession No.		3. Recipient's Catalog No.	
4. Title and Subtitle National Crash Severity Study - Quality Control Task V: Analysis to Refine Spinout Aspects of CRASH				5. Report Date January 1981	
				6. Performing Organization Code	
7. Author(s) Raymond R. McHenry and Brian G. McHenry				8. Performing Organization Report No. ZP-6003-V-4	
9. Performing Organization Name and Address Calspan Field Services, Inc. P.O. Box 400 Buffalo, New York 14225				10. Work Unit No. A09/A30	
				11. Contract or Grant No. DOT-HS-6-01442	
12. Sponsoring Agency Name and Address U.S. Department of Transportation National Highway Traffic Safety Administration 400 7th Street, S.W. Washington, D.C. 20590				13. Type of Report and Period Covered Final Report	
				14. Sponsoring Agency Code	
15. Supplementary Notes					
16. Abstract <p>The objectives of this research were to further develop the angular momentum solution mode for the CRASH program, to evaluate an alternative approach for the analysis of spinout trajectories based on the use of an average drag factor and to revise the documentation in the CRASH User's Manual, as required.</p> <p>Analysis of fifty cases selected from the NCSS program data bank indicated that many cases did not fit within the framework of simplifying assumptions on which the SPIN2 subroutine of the CRASH program is based. Consequently, modifications of SPIN2 which would yield reliable and accurate approximations of separation velocities for all cases could not be achieved. It was concluded that, rather than continue development of the empirical approximation technique which has become increasingly complicated, it would be preferable to concentrate on the existing trajectory routine, applying physical laws directly. It was also concluded that, because of the large number of interacting variables in a vehicle spinout, the development of the concept of an "average drag factor" for approximating the linear and angular velocities of a vehicle at separation from a collision was not practical. A revision of subroutine OBLIQE of CRASH3 was developed to improve the accuracy of the calculation with which the angular momentum at separation is approximated.</p> <p><u>Recommendations</u></p> <p>To achieve a general improvement in the reliability and accuracy of approximations of the angular and linear velocities at separation, a step-by-step time history form of trajectory solution should be implemented.</p>					
17. Key Words CRASH, Accident Reconstruction, Spinout Trajectories, Angular Momentum			18. Distribution Statement Document is available to the public through the National Technical Information Services, Springfield, Virginia 22161.		
19. Security Classif. (of this report) None		20. Security Classif. (of this page) None		21. No. of Pages 64	
				22. Price	

METRIC CONVERSION FACTORS

Approximate Conversions to Metric Measures				
Symbol	When You Know	Multiply by	To Find	Symbol
LENGTH				
in	inches	2.5	centimeters	cm
ft	feet	30	centimeters	cm
yd	yards	0.9	meters	m
mi	miles	1.6	kilometers	km
AREA				
in ²	square inches	6.6	square centimeters	cm ²
ft ²	square feet	0.09	square meters	m ²
yd ²	square yards	0.8	square meters	m ²
mi ²	square miles	2.6	square kilometers	km ²
	acres	0.4	hectares	ha
MASS (weight)				
oz	ounces	28	grams	g
lb	pounds	0.45	kilograms	kg
	short tons (2000 lb)	0.9	tonnes	t
VOLUME				
sp	teaspoons	5	milliliters	ml
Tbsp	tablespoons	15	milliliters	ml
fl oz	fluid ounces	30	milliliters	ml
c	cups	0.24	liters	l
pt	pints	0.47	liters	l
qt	quarts	0.95	liters	l
gal	gallons	3.8	liters	l
ft ³	cubic feet	0.03	Cubic meters	m ³
yd ³	cubic yards	0.76	Cubic meters	m ³
TEMPERATURE (exact)				
°F	Fahrenheit temperature	5/9 (after subtracting 32)	Celsius temperature	°C

1 inch = 2.54 centimeters exactly. 1 foot = 0.3048 meters exactly. 1 mile = 1.609344 kilometers exactly. 1 acre = 0.404685642 hectares exactly. 1 tonne = 1000 kilograms exactly. 1 liter = 1.056688 quarts exactly. 1 gallon = 3.785411784 liters exactly. 1 cubic foot = 0.0283168466 cubic meters exactly. 1 cubic yard = 0.764554858 cubic meters exactly.



Approximate Conversions from Metric Measures				
Symbol	When You Know	Multiply by	To Find	Symbol
LENGTH				
mm	millimeters	0.04	inches	in
cm	centimeters	0.4	inches	in
m	meters	3.3	feet	ft
m	meters	1.1	yards	yd
km	kilometers	0.6	miles	mi
AREA				
cm ²	square centimeters	0.16	square inches	in ²
m ²	square meters	1.2	square yards	yd ²
km ²	square kilometers	0.4	square miles	mi ²
ha	hectares (10,000 m ²)	2.5	acres	
MASS (weight)				
g	grams	0.035	ounces	oz
kg	kilograms	2.2	pounds	lb
t	tonnes (1000 kg)	1.1	short tons	
VOLUME				
ml	milliliters	0.03	fluid ounces	fl oz
l	liters	2.1	pints	pt
l	liters	1.06	quarts	qt
l	liters	0.26	gallons	gal
m ³	cubic meters	35	cubic feet	ft ³
m ³	cubic meters	1.3	cubic yards	yd ³
TEMPERATURE (exact)				
°C	Celsius temperature	9/5 (then add 32)	Fahrenheit temperature	°F

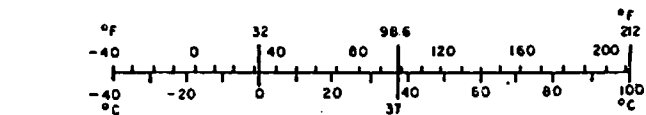


FIGURE 3. METRIC CONVERSION FACTORS

111

ZP-6003-V-4

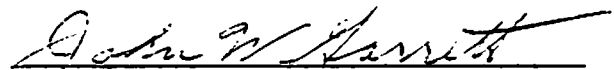
FOREWORD

The research presented in this report was performed by Research Engineers, Inc. (REI) under a subcontract with Calspan Field Services, Inc. It constitutes completion of Task V of the work statement of Contract No. DOT-HS-6-01442 with the National Highway Traffic Safety Administration (NHTSA), U.S. Department of Transportation.

The objectives of Task V of Contract No. DOT-HS-6-01442 were (1) to further develop the angular momentum solution mode for CRASH, (2) to evaluate an alternative approach for analysis of spinout trajectories, based on the use of an average drag factor, and (3) to revise and extend, as required, the related documentation in the CRASH User's Manual.

The opinions, findings, and conclusions expressed in this report are those of the authors and are not necessarily those of NHTSA.

This report has been reviewed and is approved by:



John W. Garrett
Manager
Accident Research Division

TABLE OF CONTENTS

<u>SECTION</u>		<u>PAGE</u>
1.0	Introduction.....	1
2.0	Conclusions and Recommendations.....	8
	2.1 Conclusions.....	8
	2.2 Recommendations.....	11
3.0	Discussion of Results.....	13
	<u>Task A - Damage Effects</u>	14
	<u>Task B - NCSS Case Selection</u>	19
	<u>Task C - SMAC Runs</u>	20
	<u>Task D - Regression Analysis, α_1, ρ</u>	28
	<u>Task E - Average Drag Factor</u>	49
	<u>Task F, G, H, I, and J - Comparison of Results</u>	53
4.0	References.....	54
	Appendix A.....	55
	Appendix B.....	57

LIST OF FIGURES

<u>FIGURE NO.</u>		<u>PAGE</u>
1	Run No. 3 - No Braking (\dot{S}_S FWD).	3
2	Run No. 18 - No Braking (\dot{S}_S FWD).	4
3	Run No. 8 - RF Damage.	5
4	ρ_v, ρ_ψ vs Path Ratio (PR) for cases where $\theta = 1.0$.	10
5	Effects of vehicle crush on angular momentum calculations (offset frontal).	16
6	Effects of vehicle crush on angular momentum calculations (side impact).	17
7	Angular velocity time history for cases where $\theta = 1.0$.	30
8	β and $\Delta\psi$ classification wheels.	32
9	Angular velocity time history.	35
10	Comparison of angular velocity time histories for (1) case where sign of β and $\Delta\psi$ are the same and (2) case where sign of β and $\Delta\psi$ are opposite.	37
11	Case 46. Vehicle #1 and #2 illustrating con- trast of step deceleration with similar ρ_s and β_s .	39
12	Random sampling illustrating angular velocity deceleration variations due to 0, 1, 2, 3, and 4 wheel drag.	41
13	Transition point in angular velocity time histories.	43
14	Least-squares fits of ρ vs. $S_1/\Delta\psi$.	44

1.0 INTRODUCTION

An analytical procedure for approximating the linear and angular velocities of a vehicle at the start of its motions subsequent to a collision, which is defined by Marquard in Reference 1, served as the starting point for corresponding aspects of the CRASH^{*} computer program (Ref. 2). The cited procedure (Ref. 1) takes into account the fact that the linear and angular (i.e., yaw rotation) displacements of a four-wheeled vehicle subsequent to a collision each occur under conditions of intermittent deceleration when the wheels are free to rotate. By approximating the linear and angular deceleration rates of a vehicle with either (1) all wheels freely rotating or (2) all wheels locked during the different phases of a spinout motion, Marquard developed approximate relationships between the total linear and angular displacements during the travel from separation to rest and the corresponding linear and angular velocities of a vehicle at separation from its collision partner, for the two cited cases of rotational resistance at the wheels.

In Reference 2, the relatively simple Marquard relationships were first extended to permit applications to the case of partial braking and/or damage-locked individual wheels. Evaluation of the resulting, modified relationships by means of trial applications to SMAC^{**}-generated spinout trajectories revealed several shortcomings.

^{*} Calspan Reconstruction of Accident Speeds on the Highway, Reference 2.

^{**} Simulation Model of Automobile Collisions, Reference 3.

First, it was found that a residual linear velocity frequently exists at the end of the rotational (i.e., yawing) motion. Next, it was found that the general shapes of plots of linear and angular velocity vs. time changed substantially as functions of the ratio of linear to angular velocity at separation from the collision (e.g., see Figures 1 and 2). Finally, the transitions between the different deceleration rates of the linear and angular motions were found to occur gradually rather than abruptly. Slope changes in the plots of linear and angular velocities against time were found to generally occur in the form of rounded "corners" in the curves (e.g., see Figure 3).

To improve the accuracy of the approximations of separation velocities, provision was made for the introduction of a residual linear velocity at the end of the rotational motion (see Figures 1, 2, and 3). Also, five empirical coefficients, in the form of polynomial functions of the ratio of linear to angular velocity at separation, were incorporated in the developed analytical relationships. Since the velocity ratio is initially unknown, a solution procedure was developed whereby several trial values of the ratio, based on an approximate equation, are used to obtain multiple solutions. The solution for which the velocity ratio most closely matches the trial value is retained.

The cited analytical developments, which are reported in Reference 2, involved only limited efforts which were aimed primarily at demonstrating the feasibility of the CRASH concept. A single table of polynomial functions to generate the empirical coefficients was

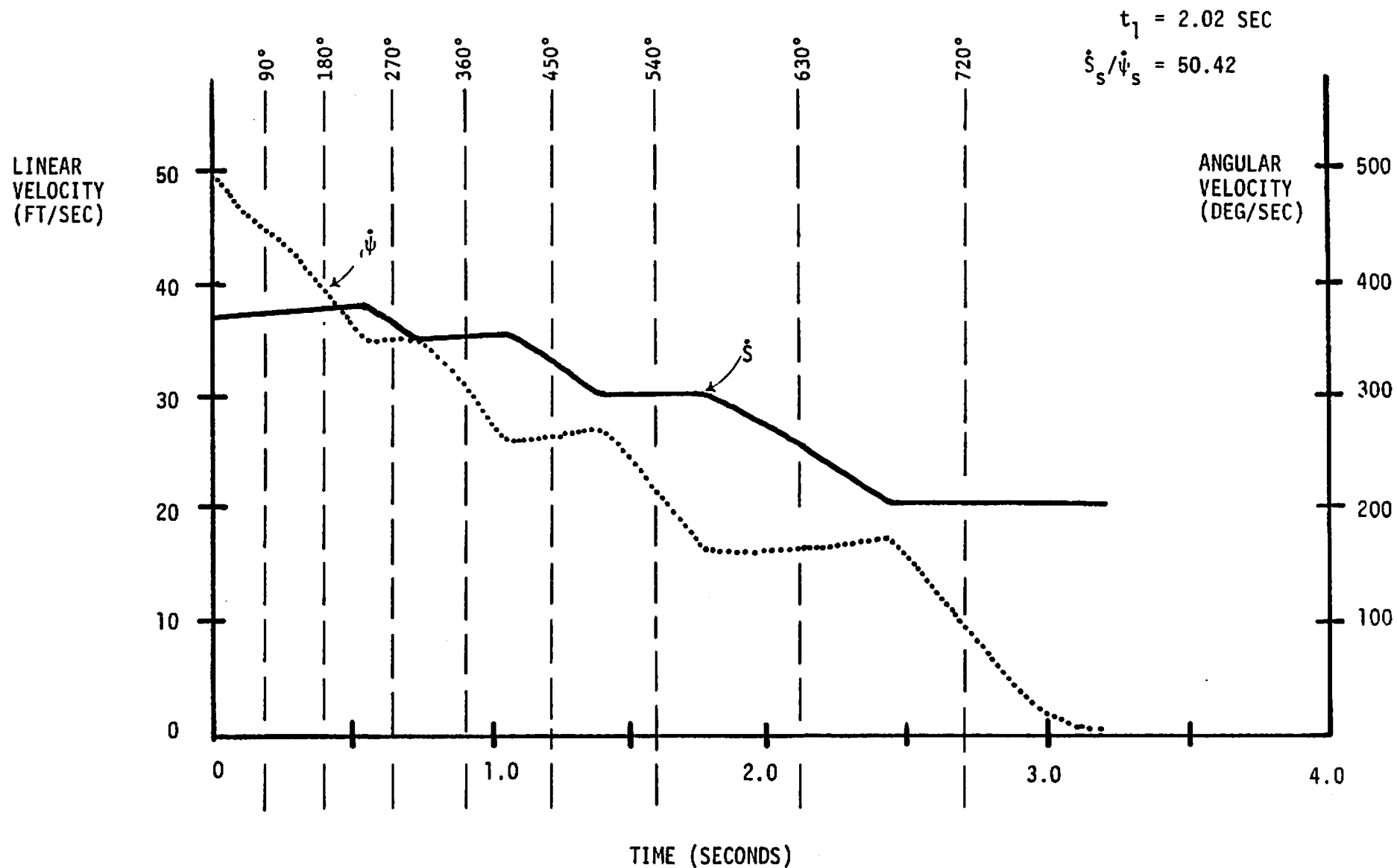


Figure 1. Run No. 3 - No Braking (\dot{s}_s FWD).

4

ZP-6003-V-4

$t_1 = 1.67 \text{ SEC}$
 $\dot{S}_s / \dot{\psi}_s = 298.8$

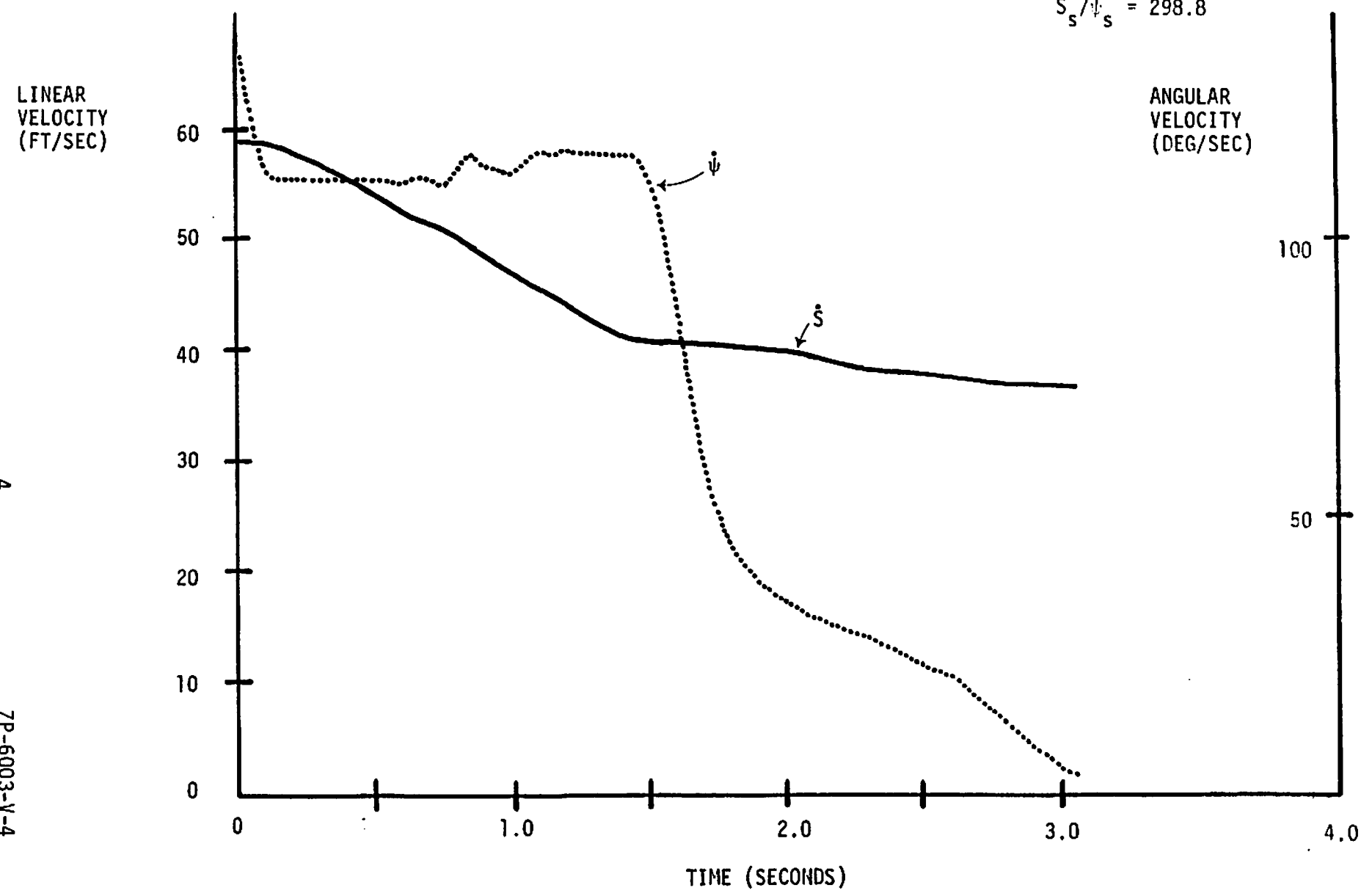


Figure 2. Run No. 18 - No Braking (\dot{S}_s FWD).

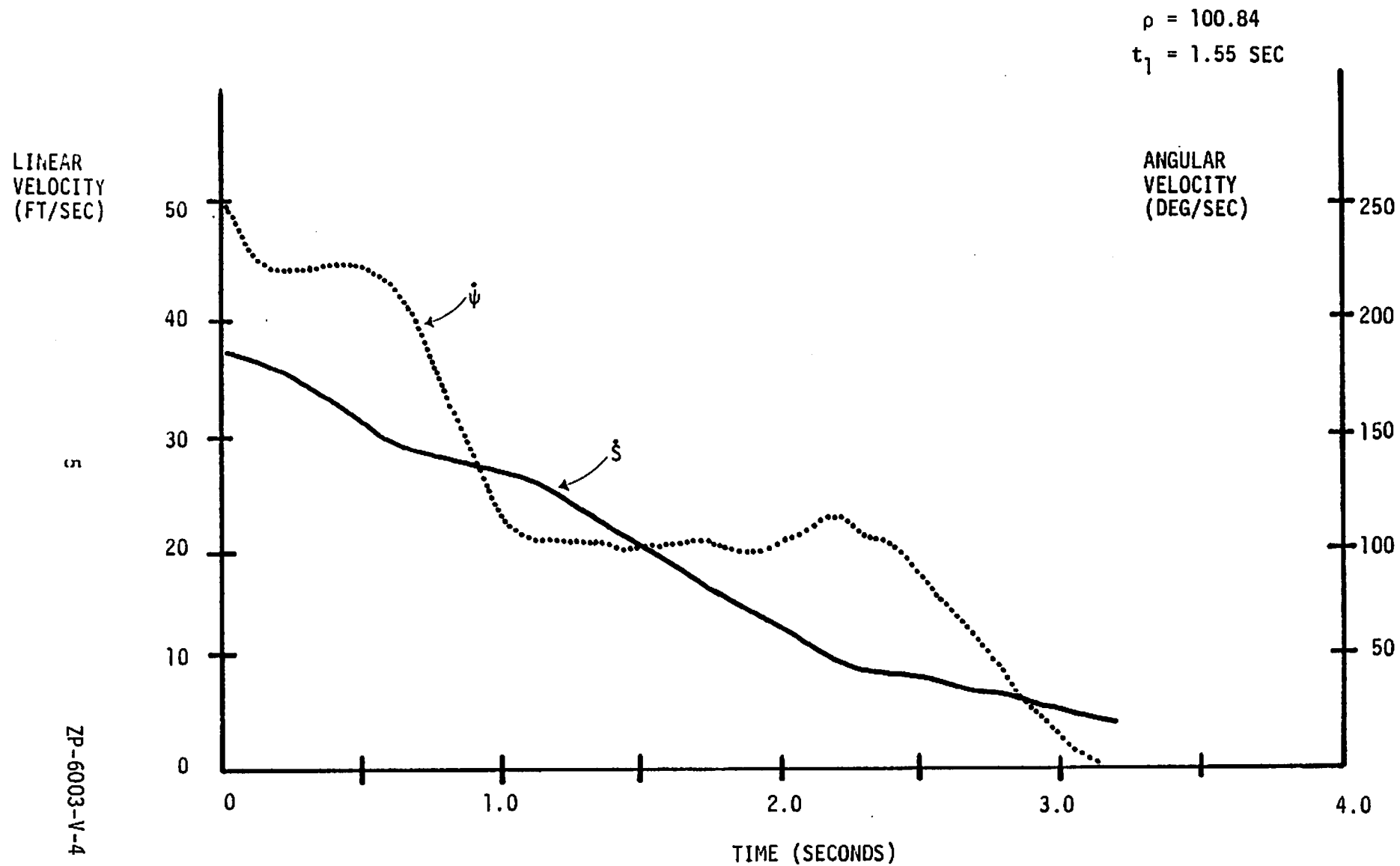


Figure 3. Run No. 8 - RF Damage.

developed, on the basis of 18 single-vehicle SMAC runs with relatively high linear and angular velocities for starting (i.e., separation) conditions.

For those 18 SMAC runs, significant improvements in the accuracy of CRASH reconstructions of the separation velocities, as compared with the original Marquard relationships, were achieved by means of the combination of the empirical coefficients and the provision for a residual linear velocity at the end of the yaw rotation. In particular, the maximum errors in the reconstructed linear and angular velocities for the 18 SMAC runs were reduced from 394% to 13.5%. The average error was reduced from approximately $\pm 70\%$ to approximately $\pm 5\%$.

In the more common, real-life accident case, a relatively small rotational (i.e., yawing) velocity may exist at separation. In such a case, the initial direction of the velocity vector with respect to the longitudinal axis of the vehicle will obviously affect the sequence and the durations of the linear and angular deceleration rates of the vehicle. Therefore, a refinement of the existing approximation technique must include the use of logical tests and more than one table of polynomial functions to generate appropriate empirical coefficients.

In view of the present complexity of the solution form for spinout motions, a practical approach toward refinements should also include an investigation of alternative solution forms. The results of such an investigation are reported herein.

The need for refinements to improve the accuracy of velocity approximations became apparent during the course of development and evaluation of angular momentum relationships reported in Reference 4. The full development and incorporation of an angular momentum form of impact-speed solution is considered to be an essential part of future development plans for the CRASH program. Accuracy problems that were encountered in the angular momentum solutions make necessary a general upgrading of the existing approximation techniques within the CRASH program.

This report documents the research approach and results of several individual tasks related to refinement of the spinout analysis aspects of CRASH. Conclusions and recommendations are presented in Section 2. Results of the research are summarized in Section 3. References are listed in Section 4.

2.0 CONCLUSIONS AND RECOMMENDATIONS

2.1 Conclusions

2.1.1 Many individual cases in the sample of SMAC-generated spinouts that were included in this investigation do not fit within the framework of simplifying assumptions upon which the SPIN2 subroutine of the CRASH program is based. As a result, modifications of SPIN2 which would yield reliable and accurate approximations of separation velocities for all cases in the sample could not be achieved.

The existing form of the SPIN2 subroutine has been demonstrated to yield an acceptable level of accuracy in approximating the linear velocity at separation, \dot{S}_s , from measured physical evidence in many applications that have involved only the conservation of linear momentum. While some accuracy problems have been recognized, particularly in cases with a small total extent of yaw rotation, the primary motivation for the reported efforts aimed at refining SPIN2 has been based on a need for increased accuracy in approximating both the angular velocity at separation, $\dot{\psi}_s$, and the linear velocity at separation, \dot{S}_s , for use in angular momentum solutions.

SPIN2 is based on a number of simplifying assumptions regarding the time histories of linear and angular velocity (e.g., see Reference 2). In the present study, it was found that some of the SMAC-generated time histories of velocities deviate markedly from those simplifying assumptions. As a result, it was not possible to "fit" the vehicle behavior to the existing simplifying assumptions by means of empirical coefficients, even with added discriminators, logic, and multiple tables of coefficients. Therefore, a significant amount of scatter remained in all of the empirical fits that were attempted.

The earlier exploratory research on this topic (Ref. 2) made use of a small number of high-energy spinouts. In the present sample of predominantly low-energy SMAC-generated spinouts, the vehicle behavior is substantially more erratic. Also, the present sample includes a larger number of variations of wheel rotational drag and combinations of linear and angular velocity at separation than were possible in the earlier research.

A realistic appraisal of the results achieved after extensive efforts leads to the conclusion that unacceptably large errors will continue to be encountered in some applications of such an empirical technique. The difficulties encountered in attempting to refine and extend the SPIN2 subroutine, combined with a recognition of ultimate limitations on the reliability of such a solution form, have raised serious doubts regarding the merits of continued development of an increasingly complicated empirical approximation technique. A more rational approach would appear to be that of focusing attention on the existing trajectory routine, in which fundamental physical laws are applied directly.

2.1.2 The large number of interacting variables in a vehicle spinout appears to preclude the successful development of an "average drag factor" concept for approximating the linear and angular velocities of a vehicle at separation from a collision.

After an extensive exploration of possible analytical approaches, it was concluded that the "average drag factor" concept could not be successfully implemented for cases other than those in which $\theta = 1$ (see Figure 4, see Section 3, Task C for symbol definitions).

Interactions among the many variables were found to preclude the development of logic and tests whereby drag coefficients, ρ_ψ and ρ_v , could be reliably predicted on the basis of measured physical evidence.

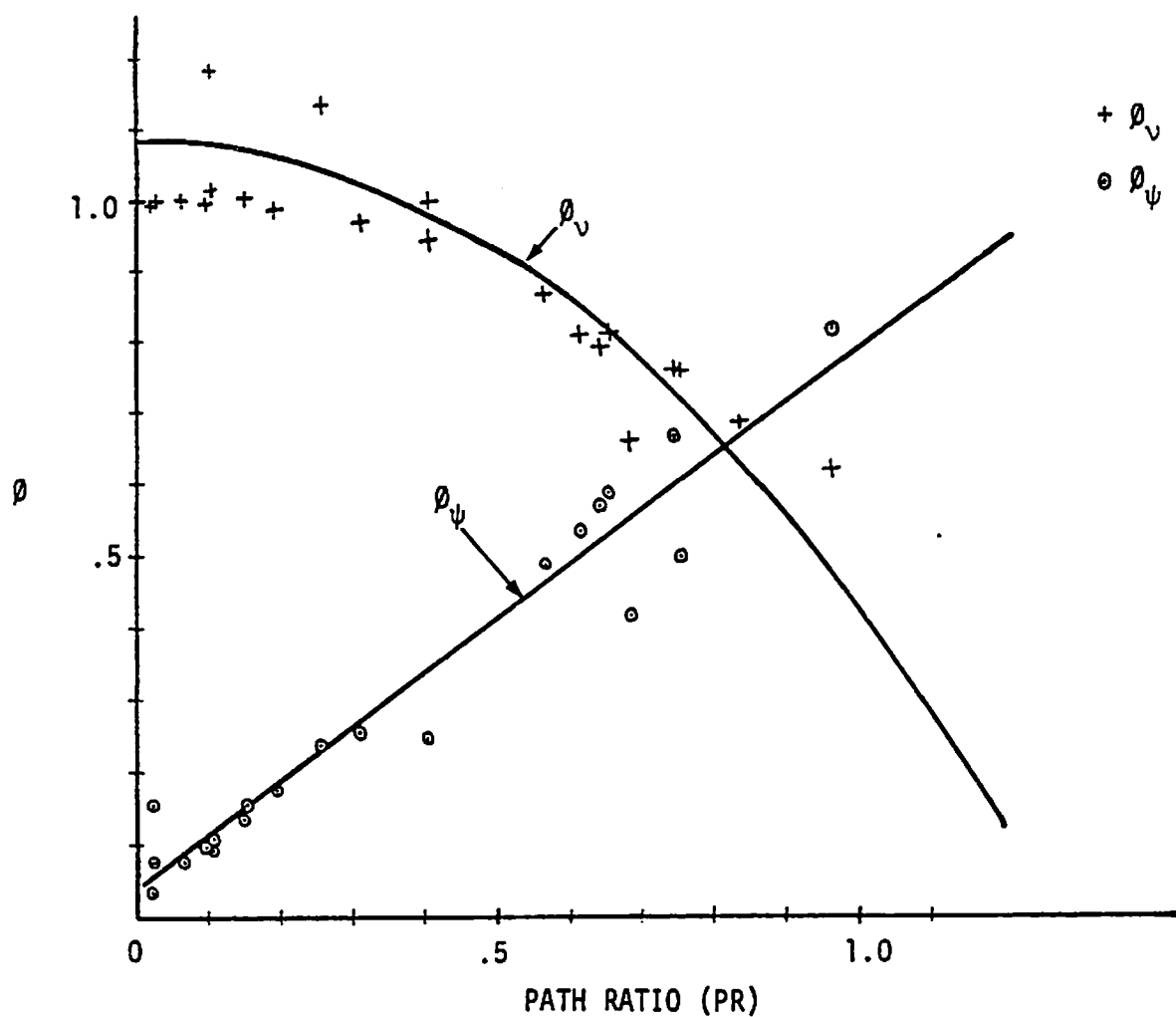


Figure 4. ρ_v , ρ_ψ vs Path Ratio (PR) for cases where $\theta = 1.0$.

The effort on this task included the development of tests of the side-slip angle at separation, β_s , and the direction and magnitude of the total rotation, $\Delta\psi$, which were aimed at prediction of "plateaus" in the time-histories of the linear and angular velocities. The relationship developed in Reference 4 for the drag factor in non-yawing skids was modified to allow an approximate integration in the presence of rotation. The definition of a path ratio (i.e., the ratio of angular to linear displacement) was modified. None of the exploratory efforts was successful in yielding acceptable predictions of drag factors, ϕ_ψ and ϕ_v .

2.1.3 A relatively simple revision has been defined for subroutine OBLIQUE of CRASH3 to improve the accuracy of calculations with which the angular momentum at separation is approximated.

The existing angular momentum calculations in subroutine OBLIQUE neglect the effects of changes in the dimensions of the two-vehicle system that are produced by vehicle crush. As a result, the magnitude of the angular momentum at separation tends to be over-estimated.

2.2 Recommendations

2.2.1 To achieve a general improvement in the reliability and accuracy of approximations of the angular and linear velocities at separation, a step-by-step time history form of trajectory solution should be implemented.

The existing trajectory subroutine of CRASH2 constitutes a direct application of fundamental physical laws. While some difficulties have been experienced with the stability of its existing logic for iterative adjustments and with the corresponding rate of convergence to an evidence match, the results of successful applications are equivalent in reliability and accuracy to trajectory calculations produced by the SMAC program. Thus, it should be possible by this means to achieve a highly accurate reconstruction of each of the SMAC-generated spinouts that has been included in the present study.

The direct application of fundamental physical laws is seen as a desirable alternative to the continued development of an increasingly complicated empirical approximation technique, particularly in view of the fact that a significant number of SMAC spinouts in the present study have been found to deviate from the simplifying assumptions on which the empirical solution form is based.

3.0 DISCUSSION OF RESULTS

When effort was initiated on the reported research program, it was recognized that a risk of possible failure to achieve the objectives existed. However, it was the genuine belief of the authors that each of the two empirical approximation techniques could be successfully developed. The late delivery of this report reflects a delay of completion that is partially due to a reluctance to abandon the task of achieving acceptable data fits.

A representative sample of realistic cases was carefully selected from the NCSS* files for use in this research. Obviously, the failure of an empirical technique to fit all of the cases reasonably well in such a sample must be recognized as a possible basis for rejection of the technique. The user of such a calculation procedure would have no way of knowing whether his specific application case corresponds to those with a reasonable fit or to those among the scatter.

A careful examination of time-history plots of linear and angular velocities for all of the cases in the sample revealed a significant number of cases in which the SMAC-predicted behavior deviated from the analytical assumptions upon which the SPIN2 subroutine is based. Attempts to accomodate such deviations by means of the use of logic and discriminators met with only partial success. As a result,

* National Crash Severity Study, Reference 5.

a realistic appraisal of residual scatter in the empirical fits has led to the conclusion that an empirical approach of the types evaluated herein will, in some applications, produce errors that will render the velocity results unacceptable for use in angular momentum relationships.

Performance of the reported research is considered to have constituted a necessary step in development of the CRASH concept. Without an actual evaluation of limitations of empirical approaches, a decision to change to a somewhat more expensive step-by-step, time-history approach might be difficult to support.

In the following paragraphs, results of the individual tasks of the research program are discussed.

Task A - Damage Effects

The actual intent of this task is somewhat obscured by the selected language in the Statement of Work, whereby the moment of inertia adjustment could be interpreted as applying to the individual vehicles. While a case could be argued for such individual-vehicle adjustments (i.e., to reflect the effects of dimensional changes produced by crush), the related discussion in Reference 4 refers specifically to the change in the moment of inertia of the two-vehicle system, about the system center of gravity, that occurs between the times of initial contact and separation. In the following, the intent of the present task has been interpreted as an adjustment of the system moment of inertia to

account for effects of vehicle crush on the system configuration at separation.

In subroutine OBLIQUE of the CRASH program, the term COBL (statement 70) defines the angular momentum of the system at separation, which is equated to that at initial contact. In COBL, components of the system linear momentum at separation are multiplied by the moment arms, about the system center of gravity, that existed at initial contact. Since substantial changes of those moment arms can occur as a result of the structural crush that occurs during the collision, the neglect of damage effects on COBL can introduce a significant error in angular momentum solutions.

For example, in Figure 5 it may be seen that the lateral velocity components of the centers of gravity of vehicles #1 and #2 at separation have moment arms about the system center of gravity that are substantially different from those at initial contact (i.e., the dimensions d_1 and d_2 in Figure 5 are substantially smaller than $(x'_M - x'_{C10})$ and $(x'_{C20} - x'_M)$, respectively). For this reason, the use of initial contact dimensions will tend to produce an overestimate of the angular momentum of the system at separation.

In Figure 6, the corresponding effects of crush in an oblique side collision are depicted. (Note that displacements relative to the system center of gravity are shown in Figure 6.) It may be seen that the moment arms of velocity components of vehicle #1 and vehicle #2 about the system center of gravity change as vehicle crush occurs.

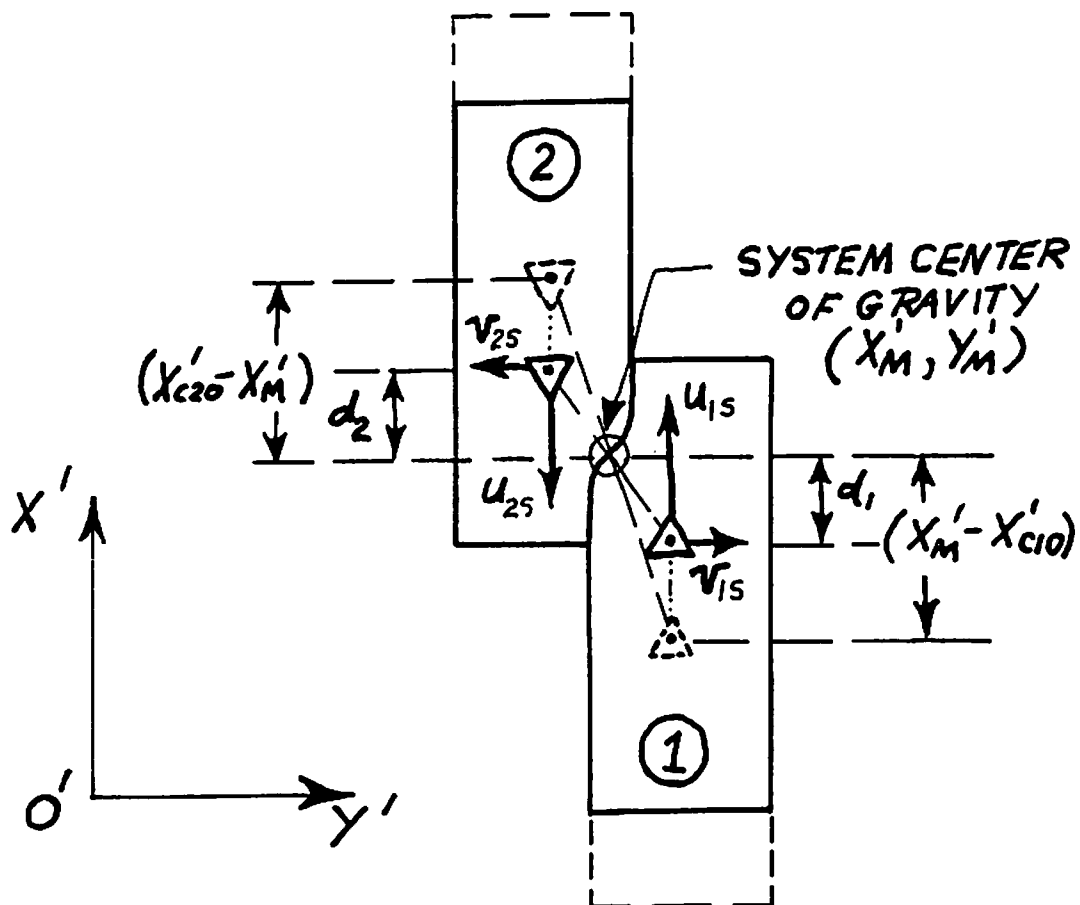


Figure 5. Effects of vehicle crush on angular momentum calculations (offset frontal).

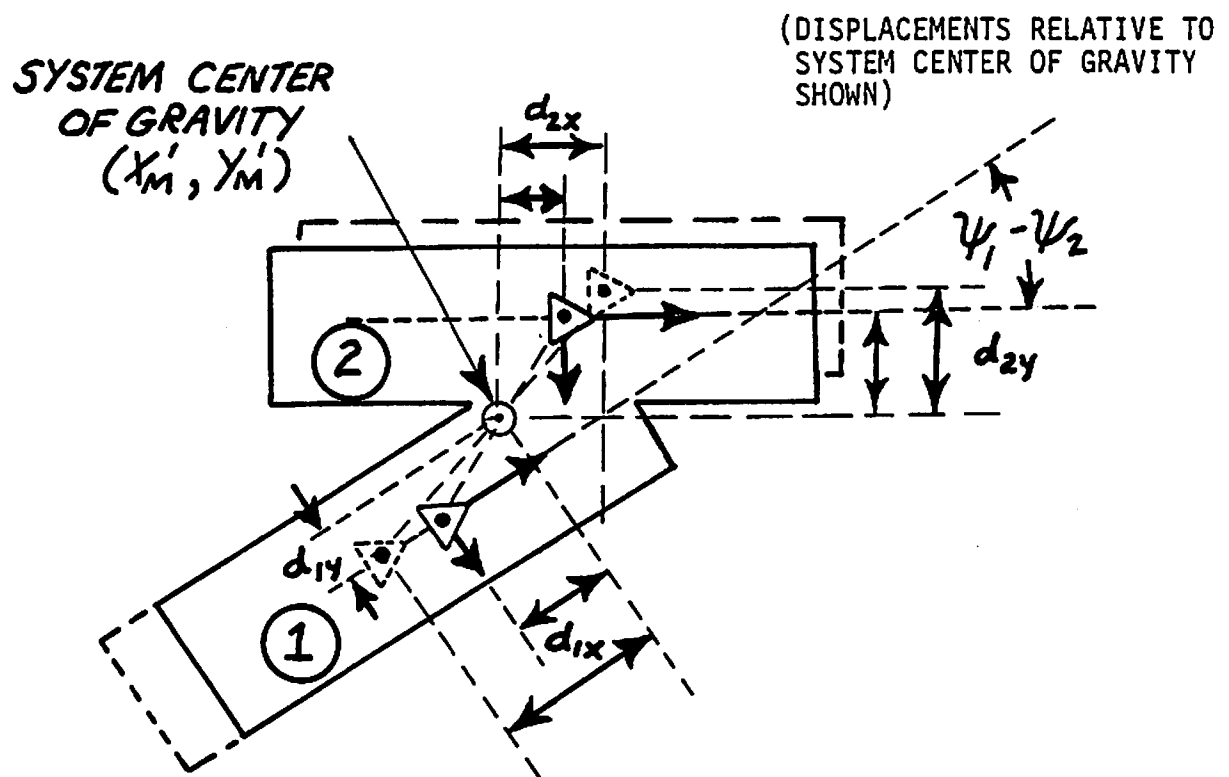


Figure 6. Effects of vehicle crush on angular momentum calculations (side impact).

The analytical approach for an approximate correction has been to make use of the average crush along the end or side of each vehicle (\bar{C}_j) and to adjust the moment arms in COBL in the following manner.

$$1.0 \quad \bar{C}_1 = \frac{\sum_{i=1}^n C_{i1}}{n}$$

$$2.0 \quad \bar{C}_2 = \frac{\sum_{i=1}^n C_{i2}}{n}$$

3.0 IF (COL 3 OF VDI FOR VEH #1 = R,L) GO TO 5.0
IF (COL 3 OF VDI FOR VEH #2 = R,L) GO TO 6.0

$$4.0 \quad \delta = \bar{C}_1 + \frac{\bar{C}_2}{|\cos(\psi_1 - \psi_2)|}$$

GO TO 7.0

$$5.0 \quad \delta = \bar{C}_1 + \bar{C}_2 |\sin(\psi_1 - \psi_2)|$$

$$\Delta X' = -\delta \sin \psi_1$$

$$\Delta Y' = -\delta \cos \psi_1$$

$$6.0 \quad \delta = \bar{C}_1 + \frac{\bar{C}_2}{|\sin(\psi_1 + \psi_2)|}$$

$$7.0 \quad \Delta X' = -\delta \cos \psi_1$$

$$\Delta Y' = -\delta \sin \psi_1$$

8.0 CORRECTION TERMS FOR COBOL,

$$\Delta(X'_M - X'_{C10}) = \left(\frac{M_2}{M_1 + M_2}\right) \Delta X'$$

$$\Delta(Y'_M - Y'_{C10}) = \left(\frac{M_2}{M_1 + M_2}\right) \Delta Y'$$

$$\Delta(X'_M - X'_{C20}) = -\left(\frac{M_1}{M_1 + M_2}\right) \Delta X'$$

$$\Delta(Y'_M - Y'_{C20}) = -\left(\frac{M_1}{M_1 + M_2}\right) \Delta Y'$$

Task B - NCSS Case Selection

The objective of the case selection procedure was to achieve a representative sample of linear and angular separation velocities in actual collisions. The criteria and the procedure for case selection were discussed on several occasions with the CTM. The NCSS files unfortunately did not contain separation conditions for the involved vehicles. Therefore, the distributions of linear and angular velocities could not be examined without repeating the CRASH2 runs for a sample of the NCSS cases. The possibilities of (1) a random selection of fifty cases or (2) a selection based on ΔV s and impact configurations were discussed.

The final selection of NCSS cases was made by the CTM.

Task C - SMAC Runs

Progress on this task was delayed for a substantial time pending the completion of selection of the 50 NCSS cases (Task B). The manual fits of Reference 2 were reviewed and data formats were planned for tabulating response variables from the spinout trajectories of the individual vehicles in SMAC runs of the NCSS cases.

Fourteen Items of Data to be Extracted from Each Spinout (i.e., 2 data sets per SMAC Run)

- (1) Note that the end of rotation is defined herein to be the first point at which the angular velocity is less than or equal to 5.0 degrees per second.
- (2) If the resultant velocity of the vehicle has not decreased to be less than or equal to 30 inches per second (2.5 ft/sec) at the end of the printout, use the final printout point as "rest" but note the magnitude of the resultant velocity in the extracted data.
- (3) In the case of multiple collision contacts, the term separation as used herein refers to the separation following the final contact.

Data Item Definitions (NOTE: All items must correspond to the same vehicle.)

- ψ_s = Heading angle of subject vehicle at point of separation, degrees.
- X'_s = X' component of CG position at separation, feet.
- Y'_s = Y' component of CG position at separation, feet.
- $\dot{\psi}_s$ = Angular velocity at separation, deg/sec.

v = Lateral velocity at point of separation, ft/sec.

u = Forward velocity at point of separation, ft/sec.

ψ_1 = Heading angle at end of rotation, deg.

X_1' = X' component of CG position at end of rotation, feet.

Y_1' = Y' component of CG position at end of rotation, feet.

v_1 = Lateral velocity at end of rotation, ft/sec.

u_1 = Forward velocity at end of rotation, ft/sec.

T_ψ = Time interval between separation and end of rotation, seconds.

ψ_R = Heading angle of subject vehicle at point of rest, degrees.

X_R' = X' component of CG position at rest, feet.

Y_R' = Y' component of CG position at rest, feet.

$\sqrt{u_R^2 + v_R^2}$ = Residual velocity at final position, if greater than 30 in/sec (2.5 ft/sec).

T_v = Time interval between separation and rest, seconds.

Inputs $\left\{ \begin{array}{l} k^2 = \text{Radius of gyration squared, in}^2. \\ A = \text{Distance between CG and front wheel centerline, inches.} \end{array} \right.$

B = Distance between CG and rear wheel centerline, inches.

μ = Tire-terrain friction coefficient.

M = Vehicle mass, lb sec²/in.

Braking Table, subsequent to time of separation.

RF = lbs.

LF = lbs.

RR = lbs.

LR = lbs.

Quantities to be Calculated and Tabulated for Each Vehicle

$$S = \sqrt{(X_R' - X_S')^2 + (Y_R' - Y_S')^2} \text{ feet}$$

$$S_1 = \sqrt{(X_1' - X_S')^2 + (Y_1' - Y_S')^2} \text{ feet}$$

$$\dot{S}_S = \sqrt{u^2 + v^2} \text{ ft/sec}$$

$$\dot{S}_1 = \sqrt{u_1^2 + v_1^2} \text{ ft/sec}$$

$$\Delta\psi = \psi_1 - \psi_S \text{ degrees}$$

$$\beta_S = \arctan \frac{v}{u} \text{ degrees}$$

$$\Delta\gamma_s = \psi_s + \beta_s - \arctan \left(\frac{Y_R' - Y_s'}{X_R' - X_s'} \right) \text{ degrees}$$

$$\theta = \frac{(RF+LF+RR+LR)}{386.4 \text{ } \mu\text{M}} \quad (\text{dimensionless})$$

$$A+B = \text{Wheelbase, inches}$$

$$\phi_\psi = \frac{k^2 \dot{\psi}_s^2}{(22139) |\Delta\psi| \mu (A+B)} \quad (\text{dimensionless})$$

$$\phi_v = \frac{\dot{S}^2}{64.4 \text{ } \mu\text{s}} \quad (\text{dimensionless})$$

$$R = \frac{(\dot{S}_s - \dot{S}_1)(\Delta\psi)}{(\dot{\psi}_s)(S_1)} \quad (\text{dimensionless})$$

$$PR = \frac{|\Delta\psi| (A+B)}{S_1 (1375.1)} \quad \begin{cases} A+B & = \text{inches} \\ \Delta\psi & = \text{degrees} \\ S_1 & = \text{feet} \end{cases}$$

$$\rho = |(\dot{S}_s / \dot{\psi}_s)| (687.54) \text{ inches/radian}$$

$$\alpha_1 = \frac{T_\psi \dot{\psi}_s}{|\Delta\psi|}$$

$$\alpha_5 = \frac{(\dot{S}_s + \dot{S}_1) T_\psi}{S_1}$$

$$\alpha_2 = \frac{2\dot{\psi}_s k^2}{(a+b)\mu g t_1 (57.2958)}$$

$$\alpha_3 \theta t_1 + \alpha_4 t_2 = \frac{(\dot{S}_s - \dot{S}_1) 12}{\mu g}$$

Definitions of Symbols

Note that the time derivative of a variable is indicated herein by a dot over the symbol for the variable.

$(a+b)$ = Wheelbase, inches.

g = 386.4 inches/sec².

k^2 = radius of gyration squared, in².

$PR = \frac{|\Delta\psi| (a+b)}{2s}$ = Path ratio of angular to linear travel, dimensionless.

$R = \frac{(\dot{S}_s - \dot{S}_1)(\Delta\psi)}{(\dot{\psi}_s)(S_1)}$ dimensionless.

s = Distance between separation and rest, inches.

S_1 = Distance between separation and end of rotation, inches.

\dot{S}_s = Resultant linear velocity at separation, inches/sec.

\dot{S}_1 = Resultant linear velocity at end of rotation, in/sec.

$t_1 = \frac{2\dot{\psi}_s k^2}{(a+b)\mu g \alpha_2}$ = Actual time of angular deceleration, seconds.

T_v = Time interval between separation and rest, sec.

T_ψ = Time interval between separation and end of rotation, sec.

β_s = Side slip angle at separation, degrees.

$\Delta\gamma_s$ = Difference between a straight line to the rest position and the actual direction of the velocity vector at separation, degrees.

θ = Decimal portion of full longitudinal deceleration
 $0 \leq \theta \leq 1.00$
(Also classify for which wheel(s) in relation to $\text{sgn } \dot{\psi}_s$.)

μ = Friction coefficient, dimensionless.

ϕ_v = $\frac{\dot{S}^2}{2 \mu g s}$ = Empirical coefficient in relationship used to approximate linear velocity.

ϕ_ψ = $\frac{k^2 \dot{\psi}_s^2}{(57.3)(a+b)\mu g |\Delta\psi|}$ = Empirical coefficient in relationship used to approximate angular velocity.

$\Delta\psi$ = Total rotation between separation and end of rotation, deg (CW = + , CCW = -).

$\dot{\psi}_s$ = Angular velocity at separation, deg/sec (CW = + , CCW = -).

Steps Used in Determining t_1 and t_2 for Calculation of α_2 , α_3 , and α_4 .

- 1.0 $\dot{\psi}_s$ vs t was plotted for each case.
- 2.0 Approximate slope lines were drawn for the different rates of deceleration. The minimum time (t) for each slope (m) was limited to values greater than 0.1 sec.
- 3.0 Tables of deceleration times were segregated into two categories:
 - (a) "straight line" deceleration
 - (b) "intermittent" or "staircase" deceleration.

"Straight line" decelerations are those in which the angular velocity decelerates at a constant rate from separation to end of rotation.

"Staircase" decelerations are those in which the angular velocity decelerates at two or more different rates. In such cases, two or more different slopes appear on the time histories.

- 4.0 For cases classified as "straight line" decelerations, the following items were recorded:

$$\theta, m, T\psi, \Delta\psi, \beta, \Delta\gamma_s, \dot{\psi}_s \text{ where } m = \Delta\dot{\psi}/\Delta t .$$

- 5.0 For cases classified as "staircase" decelerations, each slope, m , and the corresponding time, t_m , were recorded.

t_m was found by finding the intersection of the slope lines and using the corresponding time intervals on the time history plots. Although slopes near the beginning and end of a time history

plot may not intersect at the precise times of separation and end of rotation, the actual times to those events were recorded. Therefore, the value $T\psi$ is equal to the sum of the t_m 's in each time history.

In order to make the graphical interpretation procedure specific and repeatable, angular velocity "plateaus" were defined to be those time intervals, t_2 , in which the angular deceleration was less than 10 degrees per second squared. For each case, t_1 and t_2 were determined accordingly.

Utilizing the relationship:

$$\alpha_2 = \frac{2\dot{\psi}_s k^2}{(a+b)\mu g t_1 (57.296)}$$

α_2 was calculated for each case.

The individual cases were next sorted according to their ratios of linear to angular velocities, ρ , and solved simultaneously for values of α_3 and α_4 according to the following relationship:

$$\alpha_3 t_1 + \alpha_4 t_2 = \frac{(\dot{S}_s - \dot{S}_1) 12}{\mu g} .$$

In some cases, the indicated calculation was found to yield erratic and questionable results which were omitted from further calculations related to the empirical coefficients, α_3 , α_4 .

Task D - Regression Analysis, α_i , ρ

The empirical coefficients for $\alpha_i = f(\rho)$, where $\rho = \dot{S}_s / \dot{\psi}_s$, in the SPIN routine of the CRASH computer program (Reference 2, page 48) are based on manual fits to the results of only 18 single-vehicle runs of the SMAC program. In addition to inaccuracies introduced by the use of manual fits on a small sample, the original 18 SMAC runs also involved relatively high, and probably unrepresentative, linear and angular velocities for separation conditions (i.e., 25 to 40 MPH and 135 to 500 degrees/sec. at separation). Thus, the presently recognized need for refinement of $\alpha_i = f(\rho)$ should not be surprising in view of the limited prior efforts that have been applied to this fundamental aspect of the spinout portion of the CRASH program.

In relation to the recent development of angular momentum relationships for CRASH, unacceptable error levels were encountered in some sample reconstruction calculations (Reference 4). A candidate source of at least part of those errors is the table of empirical coefficients for $\alpha_i = f(\rho)$. The objectives of the present task have been to revise the coefficient table on the basis of a larger sample of more representative spinout trajectories and to obtain least-squares fits of the data points by means of a curve-fitting computer program.

The task of finding discriminators to segregate the empirical coefficients, α_i , was begun by calculating the side-slip angle (β_s), the

ratio of linear to angular velocities (ρ_s), and the amount of wheel drag (θ) at separation.

Initial efforts demonstrated that when $\theta = 1.0$, the empirical coefficients are well-behaved functions of ρ . This is due to the fact that, regardless of the heading and/or side-slip angle at separation, the vehicle is subjected to a constant drag at each wheel equal to the full friction coefficient. The time history of the angular velocity ($\dot{\psi}$) of each vehicle for the case where $\theta = 1.0$ reflects a constant deceleration rate (see Figure 7) dependent on the friction coefficient μ and the magnitude of the initial angular velocity, $\dot{\psi}$, for its slope.

However, when $\theta \neq 1.0$, there are two distinct groupings or classifications of angular deceleration. The first is similar to the cases where $\theta = 1.0$ (i.e., constant angular deceleration). The second may be classified as a "staircase" type of deceleration (i.e., the angular deceleration fluctuates between two different rates of deceleration, with a flat portion representing an angular deceleration rate approximately equal to zero, and a slanted or near-vertical portion similar to the previously discussed constant deceleration).

The corresponding empirical coefficients for these two groups were found to differ in magnitude and behavior, so discriminators were sought to differentiate the two. The cases were segregated into several groups according to the side-slip angle (β_s) and the wheel

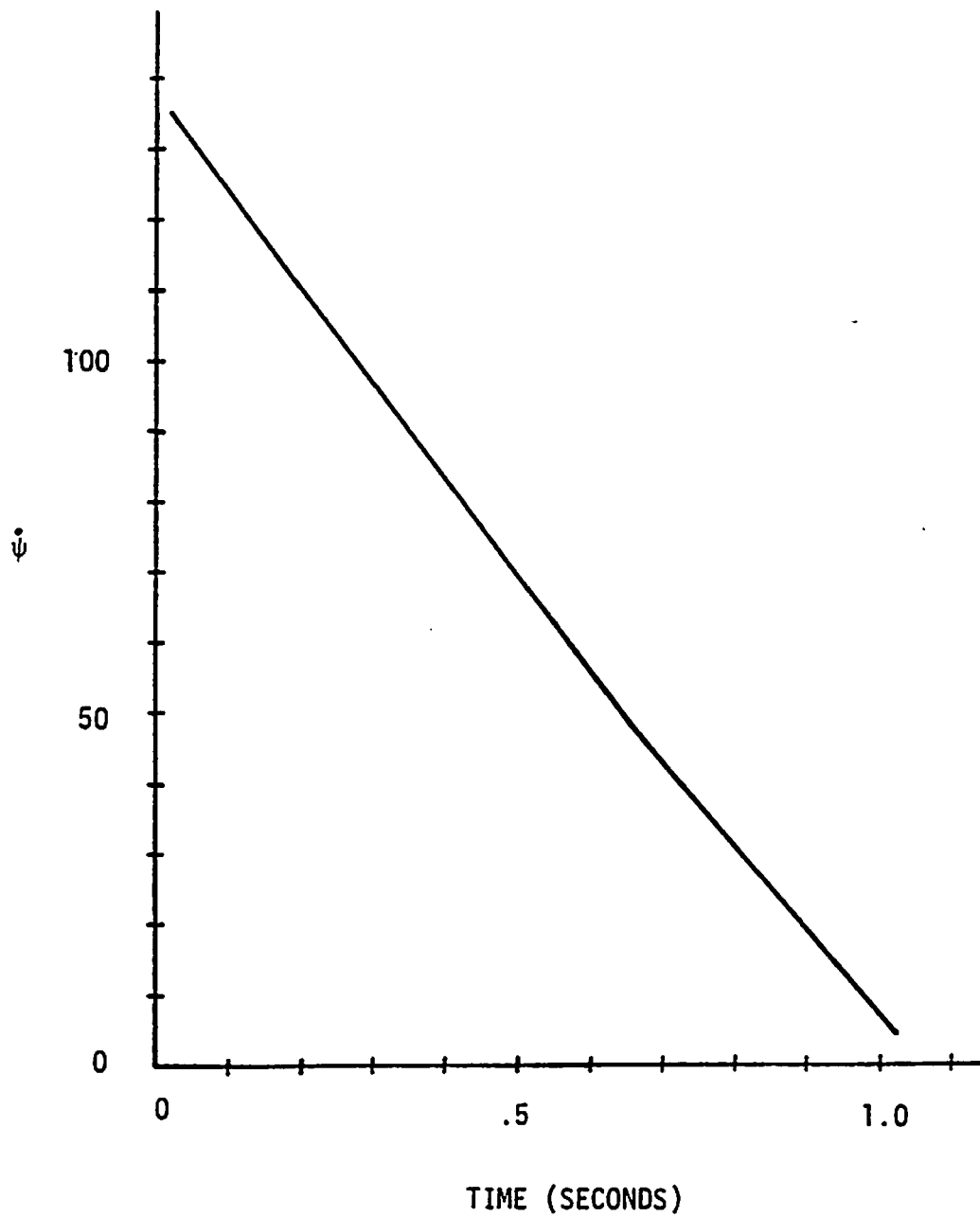


Figure 7. Angular velocity time history for case where $\theta = 1.0$.

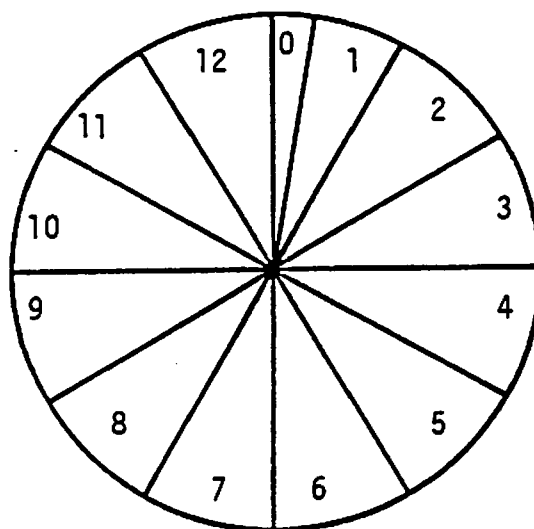
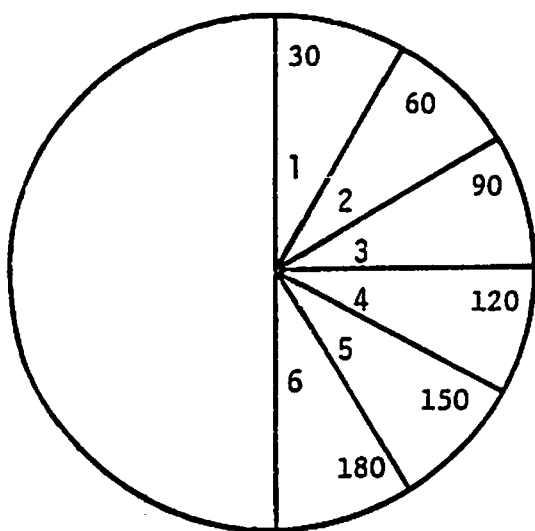
rotational resistance (θ) at separation. Several combinations of the two discriminators were tried with limited success.. A problem was found to exist in the fact that many cases, though similar in their β , θ , and ρ characteristics, differed in the characteristics of their angular velocity time histories and subsequently differed in the required magnitudes of their empirical coefficients.

The cases were next classified according to side-slip angles (β) and the total extent of rotation ($\Delta\psi$) (see Figure 8).

They were sorted into two main groupings; those with nearly lateral side-slip orientation at separation, Beta classifications 3 and 4, and those with a nearly longitudinal velocity orientation at separation, Beta classifications 1, 2, 5 and 6. The two groups were also subclassified according to their extents of rotation (i.e., magnitude of $\Delta\psi$). Several combinations of these classifications and groupings were explored, but there was found still to exist a mixture of "CONSTANT" and "STAIRCASE" deceleration types in each classification and, as a result, scatter in the magnitudes of the required empirical coefficients.

Detailed examination of the scatter cases revealed that when the directions of the side-slip angle and yaw rotation at separation are opposite, a vehicle with a nearly longitudinal side-slip angle can exhibit behavior corresponding to a predominantly

Figure 8. β and $\Delta\psi$ classification wheels.



Side-Slip, Beta (β), Classification		Magnitude of Rotation ($\Delta\psi$) Classification	
1	$0 \leq \beta < 30$	0	$0 < \Delta\psi \leq 10$
2	$30 \leq \beta < 60$	1	$10 < \Delta\psi \leq 30$
3	$60 \leq \beta < 90$	2	$30 < \Delta\psi \leq 60$
4	$90 \leq \beta < 120$	3	$60 < \Delta\psi \leq 90$
5	$120 \leq \beta < 150$	4	$90 < \Delta\psi \leq 120$
6	$120 \leq \beta < 180$	5	$120 < \Delta\psi \leq 150$
		6	$150 < \Delta\psi \leq 180$
		7	$180 < \Delta\psi \leq 210$
		8	$210 < \Delta\psi \leq 240$
		9	$240 < \Delta\psi \leq 270$
		10	$270 < \Delta\psi \leq 300$
		11	$300 < \Delta\psi \leq 330$
		12	$330 < \Delta\psi \leq 360$

lateral side-slip (i.e., an angular velocity "plateau"). Also, for most cases, vehicles with the same algebraic sign for the side-slip angle and direction of yaw rotation at separation tend to exhibit a constant angular deceleration. Subsequently, the following classifications were set up:

1. Cases where $\theta = 1.0$.
2. Cases where the sign of the side-slip angle, β_s , and the direction of the yaw rotation, $\Delta\psi$, are the same (i.e., "CONST").
3. Cases where the sign of the side-slip angle, β_s , and the direction of the yaw rotation, $\Delta\psi$, are opposite (i.e., "staircase").

The indicated three groupings exhibited a distinct stratification of the angular deceleration time histories. However, since some scatter of the empirical coefficients still existed, additional analytical discriminators were sought.

It was found that a vehicle which is at rest at the end of rotation (i.e., $\dot{S}_1 = 0$) angularly decelerates differently from a vehicle which still has linear momentum at the end of rotation (i.e., $\dot{S}_1 > 0$), and this can cause varying amounts of scatter from the main groupings. A separate table for each, therefore, was incorporated into the empirical coefficients.

When the total amount of rotation is either very small (i.e., $\Delta\psi < 10^\circ$), or when it is greater than 60 degrees, scatter was found likely to occur. The cited combinations of circumstances were not utilized as analytical discriminators because of the lack of a sufficient number of data points in each individual group (i.e., less than five points per group).

Further investigation of the scatter in the empirical coefficients revealed a sensitive relationship between the magnitudes and directions of the side-slip angle (β_s) and the angular velocity ($\dot{\psi}_s$). As a vehicle is "launched" at separation, this relationship influences its behavior to its end of rotation and rest.

A vehicle "launched" with a nearly longitudinal side-slip angle and a small angular velocity would be expected to decelerate angularly very rapidly. In contrast, a vehicle "launched" with a nearly lateral side-slip angle and a small angular velocity would be expected to have a small angular deceleration, which has been referred to herein as a "plateau" form of angular velocity. Cases 4.1 and 4.2 illustrate this contrast of angular deceleration characteristics (see Figure 9). Case 4.1, with a $\beta = 1.95$ degrees (i.e., nearly longitudinal), decelerates from -22 degrees per second to zero in 0.219 second. Whereas, case 4.2, with a $\beta = 86.93$ degrees (i.e., nearly lateral), continues rotating at 8.74 degrees per second for 1.469 seconds before coming to rest.

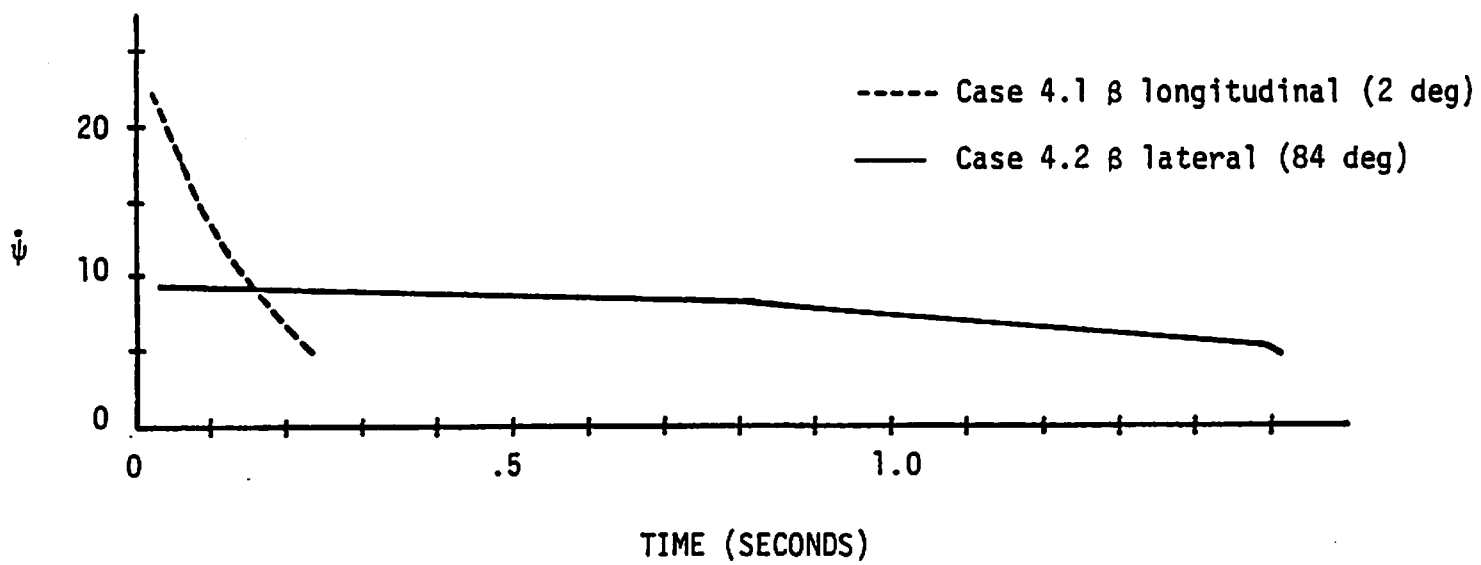


Figure 9. Angular velocity time history.

These two cases illustrate two basic forms of behavior characteristics of angular deceleration. Examination of the empirical coefficients required in these relatively simple cases (see Appendix A) illustrates the magnitudes of variations that can occur.

Vehicles launched very close to either laterally or longitudinally behave quite differently between separation and the end of rotation. The durations of the angular velocity "plateaus" are dependent on the total extent of rotation and on the rotation direction with respect to the side-slip angle at separation. Cases 5.1 and 25.2 are illustrative examples. Both cases have similar β and $\dot{\psi}$ characteristics, but they differ in their direction of angular velocities at separation. Case 5.1 has a side-slip angle of -10.2° and an angular velocity at separation of -118 degrees per second. The similarity of the signs of β_s and $\dot{\psi}_s$ allows the side-slip angle to initially decrease. The resulting angular velocity time history (see Figure 10) exhibits a constant deceleration for one-half second after separation. An angular velocity plateau is reached only when a near lateral side-slip is reached. Case 25.2, in contrast, has a side-slip angle of -24.54 degrees and angular velocity of $+162.4$ degrees per second at separation. The opposite signs cause the side-slip angle to initially increase, producing a plateau for the first three-fourths second after separation. Once a small side-slip angle is reached, a constant angular deceleration occurs. In addition, examination of case 46 reveals that vehicles No. 1 and No. 2 also illustrate

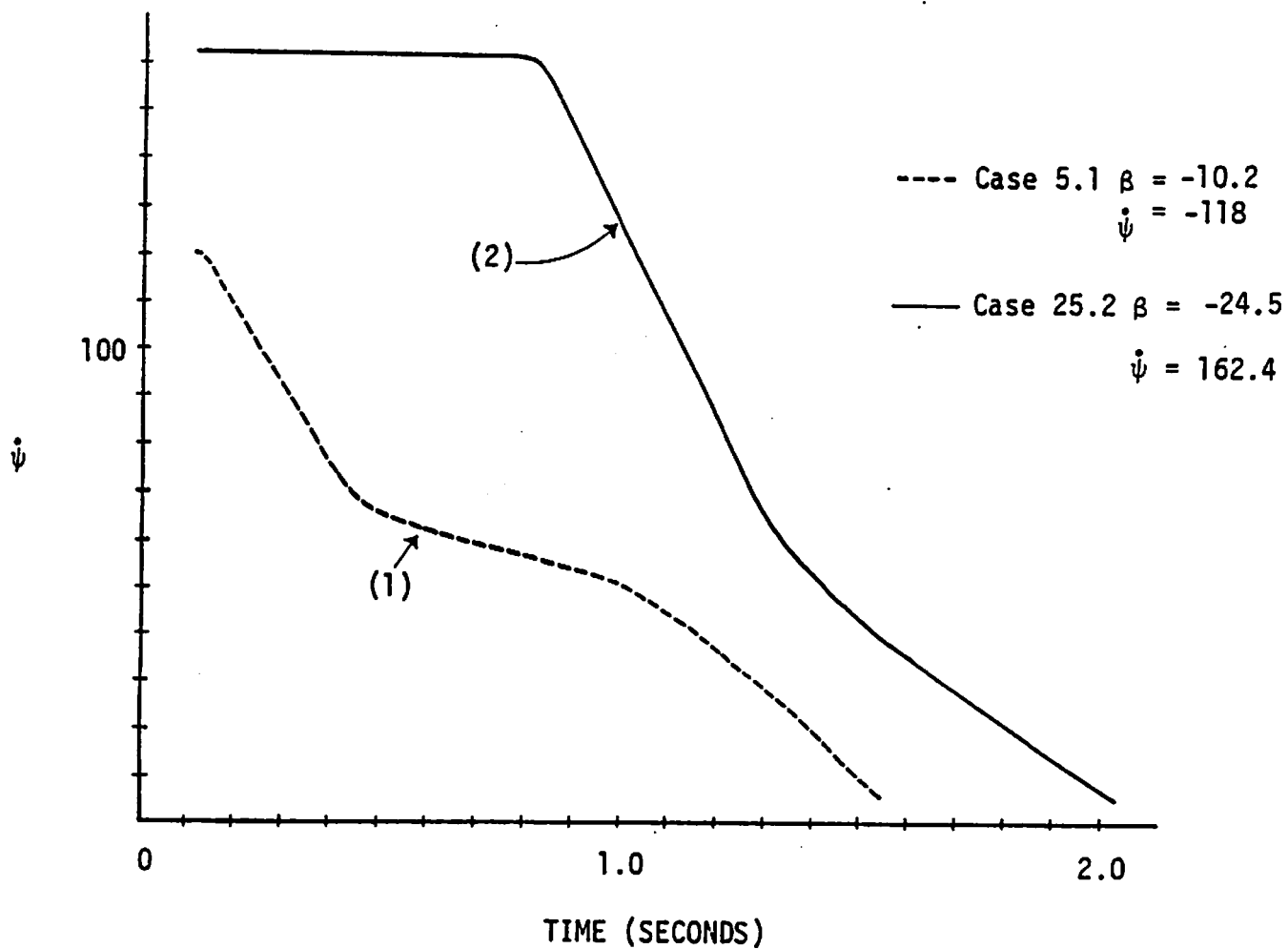


Figure 10. Comparison of angular velocity time histories for (1) case where sign of β and $\Delta\psi$ are the same, and (2) case where sign of β and $\Delta\psi$ are opposite.

this contrast of angular velocity time histories (see Figure 11), and subsequently a contrast of magnitudes of empirical coefficients.

It was concluded that cases in which the algebraic signs of side-slip angle and the angular velocity at separation are the same and those in which they are opposite require significantly different empirical coefficients.

The amount and location of wheel drag on a vehicle in a spinout also directly affects its behavior. A vehicle with all wheels locked tends to decelerate at a faster rate than one with less than all wheels locked. Also, the location of the locked wheels with respect to the velocity direction and heading (i.e., lateral vs. longitudinal) of a vehicle in a spinout affects the characteristics of its angular deceleration time history.

Differences that are related to wheel rotational drag become most apparent when either the amount of yaw rotation is greater than 60 degrees and/or the vehicle spends a significant amount of time in a near longitudinal side-slip. An imbalance of wheel drag can cause the angular deceleration rate to fluctuate, thereby causing scatter in the empirical coefficients. The scope of the reported study did not permit a detailed examination of vehicle behavior for all of the various possible combinations of wheel drag versus

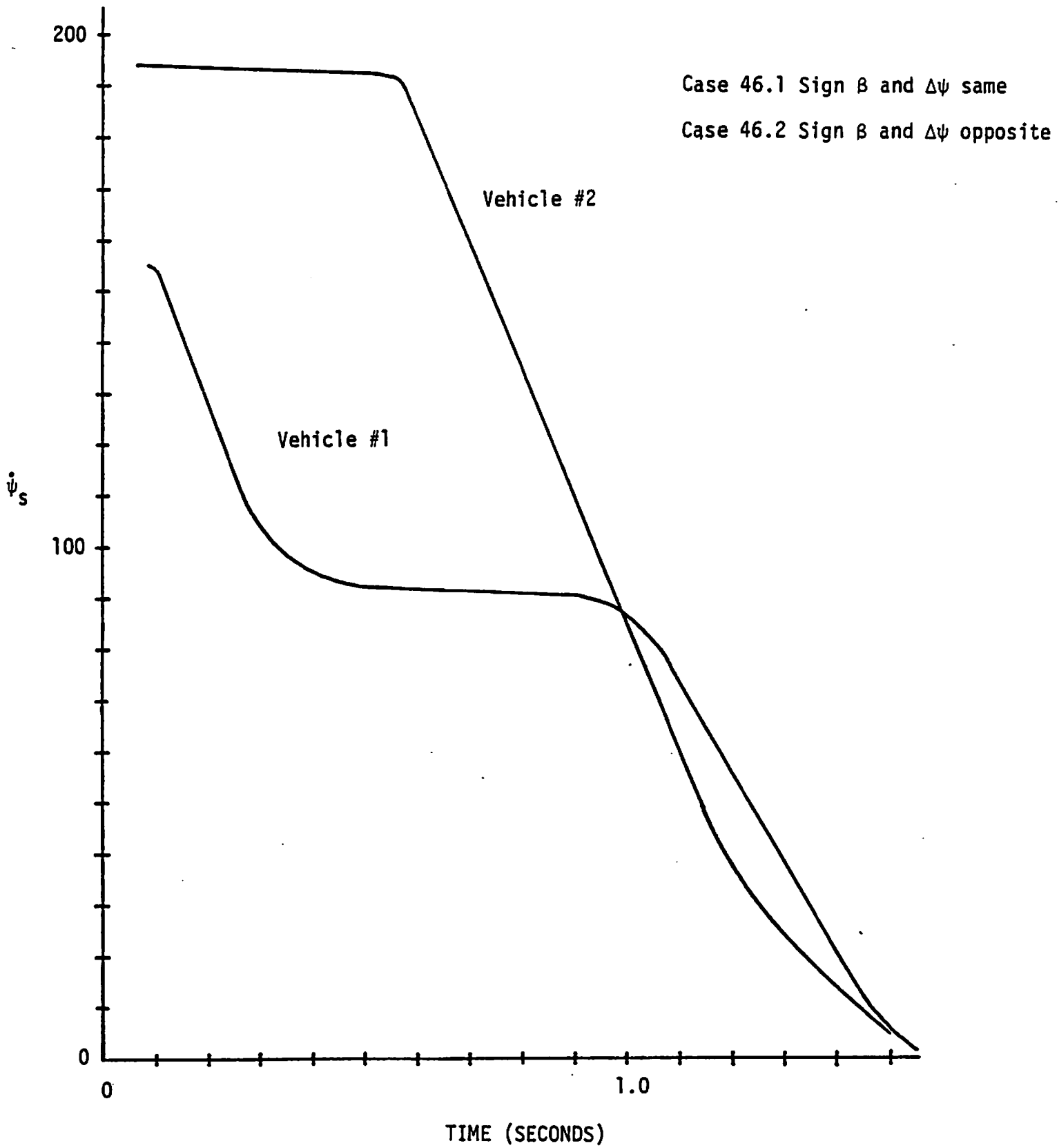


Figure 11. Case 46. Vehicle #1 and #2 illustrating contrast of step deceleration with similar ρ_s and β_s .

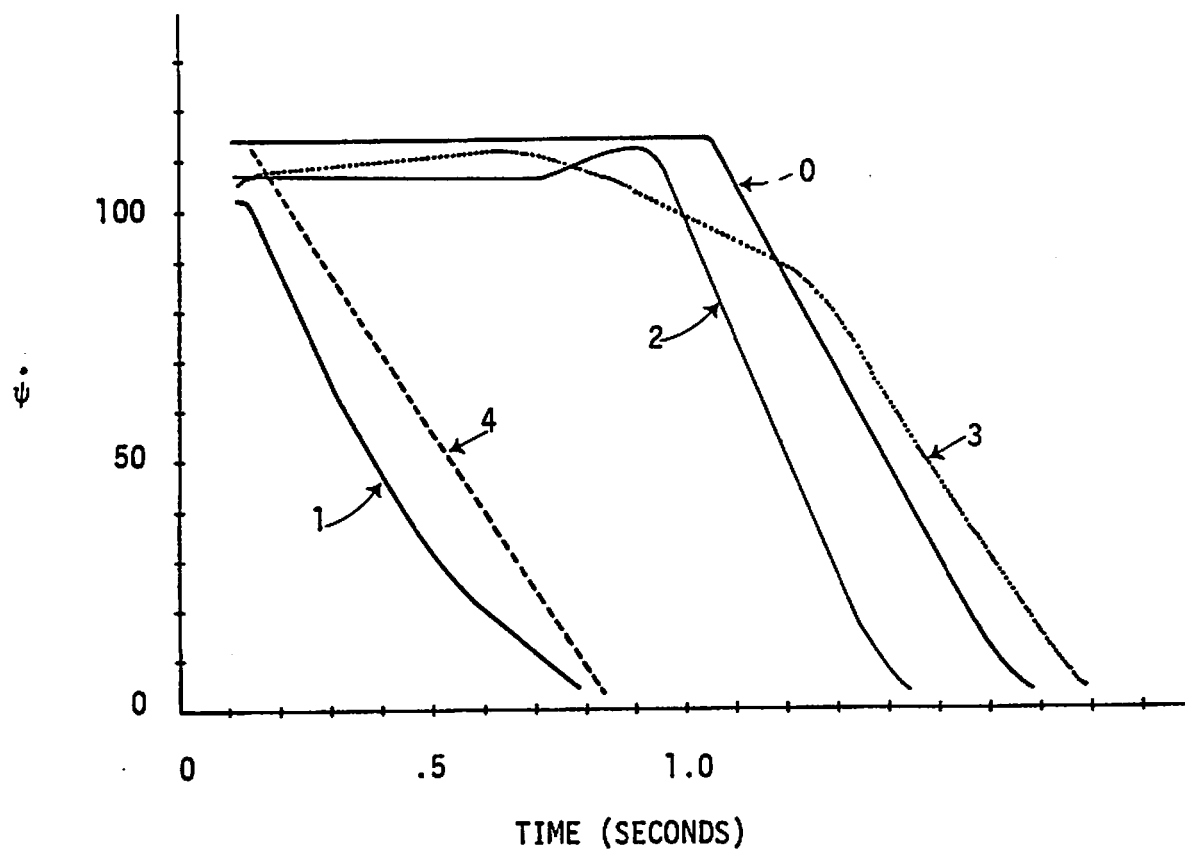
angular deceleration rates. A random sampling of angular velocity time histories for four different cases with either none, one, two, three, or four wheels with drag indicates that further investigation will be necessary before generalizations can be made (see Figure 12).

Cases were omitted in the empirical coefficient calculations for the following reasons:

1. No rotation after separation.
2. Vehicle at rest at separation.
3. Vehicles in contact prior to run start
(i.e., $ACC2 > 1.0$ at $t = 0.0$).
4. $\dot{\psi}_s$ increases after separation.

Transition Points in Angular Velocity Time Histories

As a part of the reported research effort, an investigation was undertaken to determine whether a "critical" combination of the side-slip angle, β , and the ratio of linear to angular velocity, ρ , existed for which the deceleration rate would predictably change from a velocity "plateau" to a greater value. The plotted time histories were scanned for such transition points and the corresponding times were recorded. For each case, the ratio of linear to angular velocity, ρ' , and the vehicle side-slip angle, β' , at the transition point was



Case		RF	LR	RR	LR	$\dot{\psi}_s$	β_s
0	41.1	0	0	0	0	-114.9	25.1
1	32.1	0	-623	-150	-150	-101.7	-48.4
2	5.2	0	0	-250	-390	-107.	65.6
3	6.2	0	-725	-410	-669	-106.	37.0
4	23.1	-793	-793	-731	-731	-112.8	-17.97

Figure 12. Random sampling illustrating angular velocity deceleration variations due to 0, 1, 2, 3, and 4 wheel drag.

calculated. Examination and plotting of $\beta' = f(\rho')$ indicated that an approximate relation exists whereby the transition points occur at times when $\beta \approx \frac{4000}{\rho}$ (see Figure 13).

Further examination revealed that in all cases with a constant angular deceleration:

$$|\beta_s| < |f(\rho_s)| \quad \text{and} \quad |\beta_s + \Delta\psi| < |f(\rho_s)| .$$

It was further found that the separation conditions provide a basis for prediction of the time at which a vehicle in a lateral side-slip with an angular velocity "plateau" will reach a transition point to a greater rate of angular deceleration from the relation:

$$t_2 = \frac{(4000/\rho_s) - \beta_s}{\dot{\psi}_s}$$

where t_2 is the approximate time the vehicle will remain in the condition of an angular velocity "plateau."

While the cited empirical relationship showed promise as an aid in further development of the SPIN2 procedure, it was found that some exceptions to the corresponding predictions of behavior occurred and, further, that inaccuracies in the relationship for prediction of ρ from physical evidence (Ref. 2, also see Figure 14) detracted from the reliability of transition point predictions.

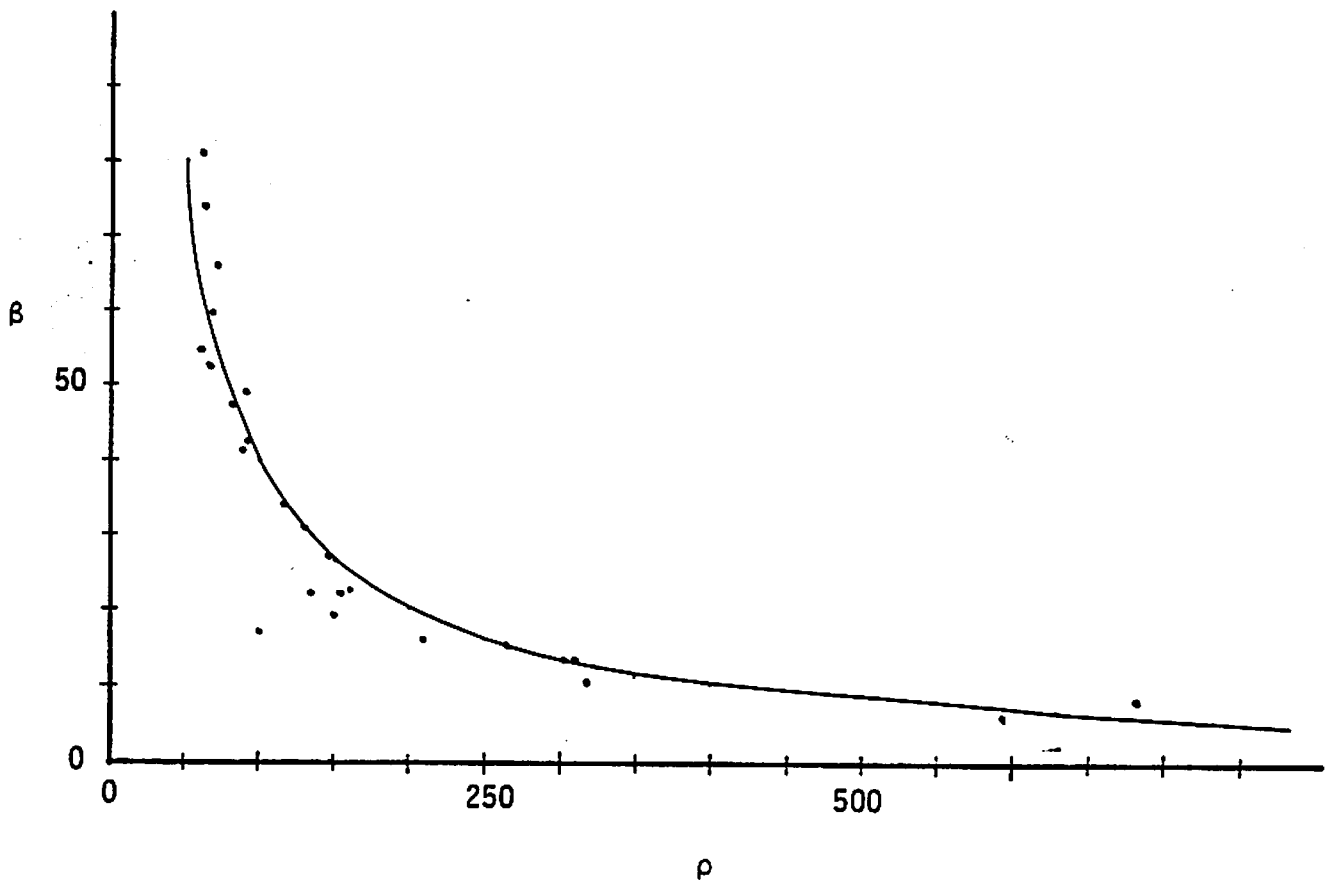


Figure 13. Transition point in angular velocity time histories.

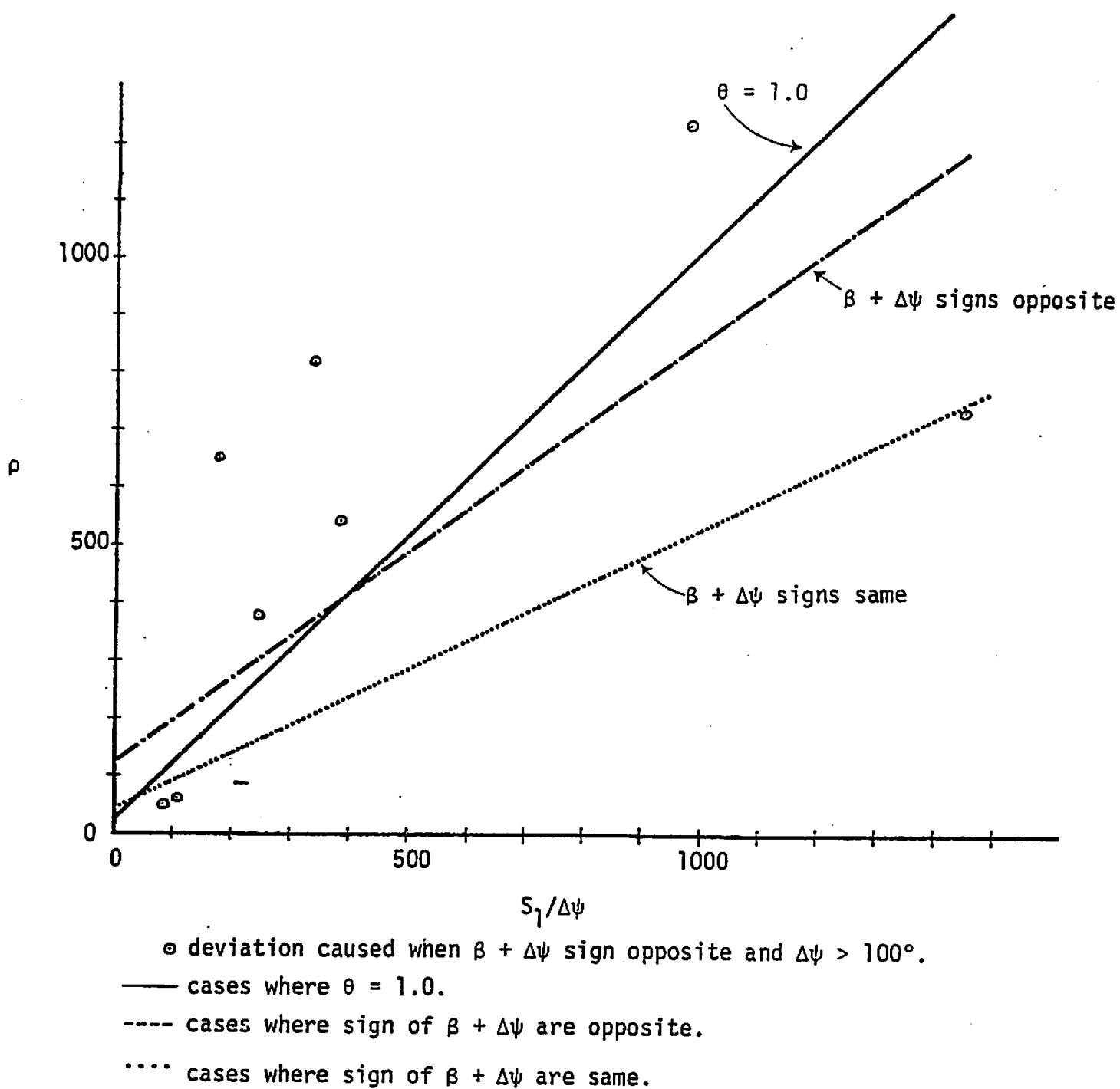
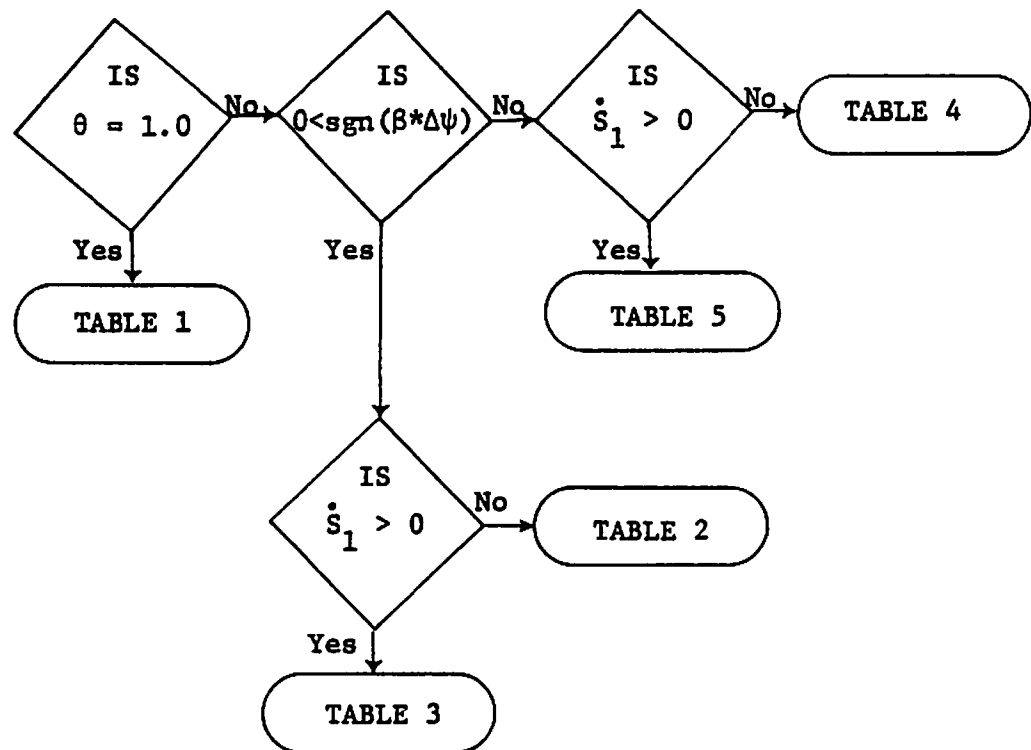


Figure 14. Least-squares fits of ρ vs. $S_1/\Delta\psi$.

Results of this research task are summarized in the following logical flow chart and tables.



EMPIRICAL COEFFICIENTS TABLES

For $\rho \geq \rho'$, $\alpha_i = k_i$

TABLE 1					
i	1	2	3	4	5
a_0	1.98227	.922981	.58194	--	2.0186
a_1	-8.05301E-4	-4.08888E-3	2.42841E-3	--	-1.97469E-4
a_2	4.43710E-7	5.49974E-6	-3.04120E-6	--	1.51185E-7
ρ'	1000	500	500	0	1000
k	1.62068	.253476	1.03587	1.0	1.97232

TABLE 2					
i	1	2	3	4	5
a_0	2.00808	.635451	3.22961	.388992	1.47389
a_1	4.05340E-4	-4.66251E-5	-1.53296E-2	3.48786E-3	4.57158E-3
a_2	--	--	--	-7.31778E-6	--
ρ'	200	500	150	250	250
k	2.08915	.612138	.93017	.803596	2.61678

EMPIRICAL COEFFICIENTS TABLES

For $\rho \geq \rho'$, $\alpha_j = k_j$

TABLE 3					
i	1	2	3	4	5
a_0	2.35308	.844074	1.08083	.388992	1.95498
a_1	-4.65774E-3	-7.65937E-4	8.25837E-4	3.48786E-3	7.69472E-4
a_2	5.62502E-6	6.44980E-7	--	-7.31778E-6	-9.63865E-7
ρ'	700	800	500	250	800
k	1.84892	.644112	1.49375	.803596	1.95368

TABLE 4					
i	1	2	3	4	5
a_0	1.92056	.7011	2.23588	1.12444	2.02359
a_1	-1.49121E-3	-5.15854E-4	-9.08942E-3	-4.63094E-4	3.16247E-5
a_2	--	--	1.55996E-5	--	--
a_3	--	--	-6.83792E-9	--	--
ρ'	800	800	800	800	500
k	1.95368	.288417	1.44707	.753965	2.04889

EMPIRICAL COEFFICIENTS TABLES

For $\rho \geq \rho'$, $\alpha_i = k_i$

TABLE 5					
i	1	2	3	4	5
a_0	2.0271	.894641	2.23588	1.12444	2.24184
a_1	-4.36705E-3	-6.66111E-4	-9.08942E-3	-4.63094E-4	1.78853E-4
a_2	7.37863E-6	--	1.55996E-5	--	-3.38454E-7
a_3	-3.42962E-9	--	-6.83792E-9	--	--
ρ'	1000	500	800	800	500
k	1.60906	.561586	1.44707	.753965	2.24665

Task E - Average Drag Factor

In the initial form of the SPIN routine of the CRASH computer program, separate calculation procedures were included for the cases of (1) locked wheels and (2) partial or no braking. Each procedure was based on relationships defined by Marquard in Reference 1. However, it should be noted that Marquard's relationships did not include partial braking but only the cases of fully locked and freely rotating wheels.

As further development and refinement of SPIN was undertaken (Ref. 2), it was found that extended relationships which were developed to include the case of partial braking yielded results, for the limiting case of locked wheels, that were equivalent in accuracy to those obtained with the separate locked-wheel relationships. Therefore, the locked-wheel relationships were eliminated from SPIN.

The Marquard approach for locked-wheel relationships, whereby empirical coefficients are applied directly in separate calculations of linear and angular velocities, is attractive for consideration of further development for the case of partial braking because of its relative simplicity. The "average drag factor" computations within the present task are based on an extension of the cited locked-wheel relationships, as outlined in the following.

Original Form Of Locked-Wheel Relationships (Based on Reference 1)

Inputs: X'_{CR}, Y'_{CR}, ψ_R = Rest position and orientation, feet and degrees.

X'_{CS}, Y'_{CS}, ψ_S = Position and orientation at separation, feet and degrees.

$a + b$ = Wheelbase, inches.

k^2 = Radius of gyration squared for complete vehicle in yaw, in².

μ = Nominal tire-ground friction coefficient.

g = Acceleration of gravity, inches/sec².

$$1.0 \quad S = 12 \sqrt{(X'_{CR} - X'_{CS})^2 + (Y'_{CR} - Y'_{CS})^2} \quad \text{inches}$$

$$2.0 \quad \Delta\psi = \frac{(\psi_R - \psi_S)}{57.3} \quad \text{radians}$$

$$3.0 \quad \gamma_S = \arctan \left(\frac{Y'_{CR} - Y'_{CS}}{X'_{CR} - X'_{CS}} \right) \quad \text{degrees}$$

$$4.0 \quad PR = \frac{|\Delta\psi|(a+b)}{2S} \quad (\text{path ratio})$$

$$5.0 \quad \phi_\psi = \begin{cases} 0.78 (PR) - 0.16 (PR)^2, & \text{for } PR < 1.50 \\ 0.80, & \text{for } 1.50 \leq PR \end{cases}$$

$$6.0 \quad \phi_v = \begin{cases} 1.00 - 0.10 (PR) - 0.28 (PR)^2, & \text{for } PR < 1.50 \\ 0.20, & \text{for } 1.50 \leq PR \end{cases}$$

$$7.0 \quad \dot{\psi}_S = 57.3 \left(\sqrt{\frac{\theta \psi (a+b) \mu g |\Delta \psi|}{k^2}} \right) \text{sgn } \Delta \psi \text{ deg/sec}$$

$$8.0 \quad \dot{S} = \sqrt{2 \theta_v \mu g S} \text{ inches/sec}$$

$$9.0 \quad \mu_S = \dot{S} \cos (\gamma_S - \psi_S) \text{ inches/sec}$$

$$10.0 \quad v_S = \dot{S} \sin (\gamma_S - \psi_S) \text{ inches/sec}$$

The functional forms of the empirical coefficients defined in steps 5.0 and 6.0 above were extended to include the following variables.

PR = Path Ratio, ratio of distances traveled by wheels in rotational (yawing) and linear motions = $\frac{|\Delta \psi| (a+b)}{2S}$.

β_S = Side-slip angle (i.e., angle between heading direction and velocity vector) at separation, radians.

θ = Decimal portion of full longitudinal deceleration produced by wheel rotational resistance (i.e., braking and/or damage at wheels), $0 \leq \theta \leq 1.00$.

$\text{sgn } \dot{\psi}$ = Sign of angular (yawing) velocity about a vertical axis through the vehicle center of gravity, (+) CW or (-) CCW.

From the 50 selected SMAC runs, the above variables were tabulated for application in empirical relationships of the following form.

$$\phi_v = f_1 (\pm \beta, \theta, \operatorname{sgn} \dot{\psi}, PR)$$

$$\phi_\psi = f_2 (\pm \beta, \theta, \operatorname{sgn} \dot{\psi}, PR)$$

The required values of ϕ_v and ϕ_ψ for the 100 trajectory cases were determined from the relationships given in steps 7.0 and 8.0 in the preceding calculation procedure (see Appendix B).

An extensive effort was applied to the task of approximating "average drag factors," ϕ_v and ϕ_ψ , on the basis of measurable physical evidence. However, no simple rules were found with which average linear and/or angular deceleration levels of a vehicle with less than full wheel lockup (i.e., $\theta < 1.0$) could be reliably predicted. Attempts to make use of the side-slip angle, β , and the direction and magnitude of yaw rotation, $\Delta\psi$, and the path ratio, PR, were unsuccessful in achieving predictions of "average drag factors" that were reliable and accurate for all cases in the sample.

Tasks F, G, H, I, and J - Comparison of Results Obtained
With Different Empirical Solution Procedures, Corresponding
Revisions of CRASH Manual

A comparison of application results for analytical techniques to have been developed under Tasks D and E was precluded by a failure to achieve acceptable accuracies in all cases of the selected sample with either of the two forms of empirical relationships. Of great importance in relation to this finding was the fact that the sample of accident cases had been carefully selected to be representative of real-life applications.

After an extensive application of effort, it became necessary to reluctantly conclude that neither form of empirical solution procedure could produce reliably accurate approximations in all of the representative cases. Therefore, a realistic appraisal of the achieved results led to the recommendation that future developments of CRASH should focus attention on the existing step-by-step, time-history form of trajectory analysis, in which fundamental physical laws are applied directly.

The results of the reported research do not provide a basis for revisions of the CRASH User's Manual.

1. Marquard, E., "Progress in the Calculations of Vehicle Collisions," Automobiltechnische Zeitschrift, Jahrg. 68, Heft 3, 1966, pp. 74-80.
2. McHenry, R. R., "User's Manual for the CRASH Computer Program," Calspan Report No. ZQ-5708-V-3, Contract No. DOT-HS-5-01124, January 1976.
3. McHenry, R. R., "A Computer Program for Reconstruction of Highway Accidents," paper presented at the 17th Stapp Car Crash Conference, November 12-13, 1973.
4. McHenry, R. R. and J. P. Lynch, "Revision of the CRASH2 Computer Program," Final Report on Tasks 5, 6, and 7, Contract No. DOT-HS-6-01442, Calspan Report No. ZP-6003-V-1, May 1978.
5. Kahane, C. J., et al, "The National Crash Severity Study," Sixth International Technical Conference on Experimental Safety Vehicles (1976) 495-516.

APPENDIX A

Case #	Ver. #	S ₁	S ₂	S ₃	a ₄	S ₅	0	c	a ₁	a ₂	a ₃	a ₄	a ₅	t ₁	t ₂	t ₃	t ₄	
1	1	8.01	21.49	10.13	-3.61	10.19	1.0	1258.5	1.644			.9960	1.9975	0.	.9960	.506	.7	-11.74
	2	32.52	31.97	0.	131.3	-6.02	.486	659.08	.5457	.1574	.5737	.7061	2.1144	.235	.615	2.151	.7	37.31
3	1	1.598	9.774	8.88	-3.54	-4.81	.154	185.2	1.7855	.9799	1.594		2.0316	.174	0	.174	.65	-36.32
	2	58.18	47.27	14.78	-165.75	13.48	.154	379.7	1.028	.7175			2.1566	.51	1.615	2.125	.65	-80.12
4	1	5.54	26.16	24.09	-2.62	1.952	.4	792.3	1.9344	.439	1.048		1.9857	.219	0	.219	.70	-22.72
	2	84.68	74.04	41.33	11.45	86.93	.38	5824.4	1.121			.0823	1.9844	0.	1.469	1.469	.70	8.74
5	1	17.25	22.00	0.	-78.47	-10.19	.52	128.19	2.1778	.6771	1.2713	.7081	1.9546	.808	.61	1.418	.65	-118.0
	2	33.84	37.39	17.99	-114.04	65.61	.39	240.21	1.23	.6740	.8993	1.6038	2.157	.475	.843	1.318	.65	-107.02
6	1	13.15	16.46	0.	-135.8	-26.830	.43	58.46	2.15	.6891	1.4759	.5905	1.896	1.245	.25	1.515	.68	-193.57
	2	43.28	42.65	12.15	-277.71	37.29	.65	276.45	1.236	.3973	1.8394		2.1082	1.165	0.	1.665	.68	-106.07
7	1	7.11	16.47	13.41	-26.68	-22.58	.26	99.31	2.036	.9728	1.0335		1.9794	.471	0.	.471	.75	-114.02
	2	21.58	33.97	2.99	-96.34	43.40	.13	366.08	1.045	.5251	.8169	.9908	2.650	.315	1.261	1.576	.75	-43.80
9	1	7.59	14.89	0.	-68.36	-38.51	1.0	75.70	1.990	.6648	.7663		1.9736	1.006	0.	1.006	.60	-135.23
	2	30.73	37.63	15.10	9.22	17.64	1.0	2384.4	1.372			1.00	2.001	0.	1.166	1.166	.60	10.85
10	1	11.59	19.10	0.	112.54	22.54	1.0	81.55	1.970	.5059	.6629		2.269	1.377	0.	1.377	.65	161.05
	2	69.60	44.18	0.	142.36	-12.68	.154	821.63	.8315	.2815	1.6765	.7522	2.033	.609	2.597	3.202	.65	36.97
11	1	5.31	8.87	6.32	31.58	42.21	.20	63.57	2.032	.6474	1.1607		1.989	.669	0.	.669	.51	95.93
12	1	1.39	11.36	0.	23.75	28.44	1.0	99.65	1.8215	.5861	.875		1.850	.552	0.	.552	.73	78.37
	2	8.83	20.45	0.	-14.63	-33.65	1.0	453.56	1.657	.1657	1.112		1.8111	.782	0.	.782	.73	-31.0
14	1	4.78	25.33	21.71	-1.83	31.95	.692	1377.5	1.4090	.3225	1.3731		2.00			1.384	.58	-12.64
	2	15.60	30.49	23.55	3.00	18.19	.485	11583.3	.3584	.1657		.6256	1.83			.594	.58	1.81
16	1	17.76	30.44	2.81	21.93	4.30	1.0	584.93	1.7507			1.0	2.00	0.	1.073	1.073	.85	35.78
	2	2.48	14.26	13.08	2.90	15.0	.144	374.35	1.6527	.5030	1.74		2.0174	.183	0.	.183	.80	26.19
17	1	7.06	16.06	0.	-56.64	-18.55	1.0	89.95	1.9635	.5743	.785	0.	2.061	.906	0.	.906	.70	-122.75
	2	18.30	29.40	21.39	32.60	53.55	.143	163.95	1.3050	.7039	.8741	.6982	2.126	.313	.453	.764	.70	55.54
18	1	.6930	3.05	0.	-8.96	-46.60	.143	38.64	2.0654	.6852	2.773	0.	1.507	.341	0.	.341	.70	-54.27
	2	14.95	50.81	48.85	7.06	8.83	.142	750.14	1.9655	.6558	2.034		2.007	.301	0.	.301	.70	46.57
19	1	17.08	27.32	0.	55.67	20.267	1.0	249.88	1.8310	.2598	1.043	0.	2.170	1.356	0.	1.356	.60	75.17
	2	22.50	17.47	0.	-195.83	-93.48	.868	59.51	3.4331	.6024			2.586	1.57	1.761	3.331	.60	-201.83
20	1	8.61	12.44	10.13	51.76	43.60	.17	61.98	2.010	.8576	.9343	0.	1.9745	.754	0.	.754	.60	137.99
	2	10.53	25.62	23.51	-14.54	-18.78	.17	298.61	1.7808	.6917	1.476	0.	2.025	.434	0.	.434	.60	-58.99
21	1	13.31	14.63	5.09	109.46	37.027	.143	51.83	2.435	.5585	2.1557		2.034	1.373		1.373	.70	194.09
	2	40.67	38.28	8.84	143.18	-24.53	.143	311.65	1.134	.6493			2.228	.55	1.373	1.923	.70	84.45
22	1	17.72	27.61	4.79	-15.18	-3.509	1.0	824.27	1.8613			.995	2.002	0.	1.095	1.095	.65	-23.03
	2	41.23	39.04	15.64	-129.33	70.75	.52	247.32	1.3544	.5130	.8169	.9908	2.1405	.25	.764	1.614	.65	-100.53
23	1	5.55	15.20	0.	-41.13	-17.97	1.0	92.64	1.9553	.5977	.830		1.947	.771	0.	.771	.80	-112.81
	2	13.82	26.22	0.	48.7	55.928	1.0	223.19	1.4934	.2980	.9569		1.937	1.221		1.021	.80	80.77
24	1	12.94	23.24	2.84	-15.28	-8.04	1.0	630.06	1.636			.9884	1.989	0.	.986	.986	.65	-25.36
	2	9.14	24.32	23.0	8.29	2.29	.154	279.47	2.589	1.5518	1.0611		1.9984	.326	0.0	.386	.65	59.83
25	1	74.88	47.96	0.	134.29	-1.195	.414	540.92	1.398	.6733			1.972	.425	2.654	3.079	.65	60.96
	2	40.28	33.21	14.96	191.55	-24.54	.153	140.62	1.614	1.4783	1.4116	.5465	2.277	.57	1.394	1.904	.65	162.38
26	1	20.41	27.93	0.	-38.84	3.40	1.0	395.69	1.782	.3709	1.014		1.951	1.426	0.	1.426	.60	-48.53
	2	27.70	23.63	0.	-265.89	63.29	.226	68.128	1.995	.6754	1.6913	.1577	1.900	1.746	.48	2.226	.60	-238.47
28	1	10.04	18.95	12.42	-24.51	-37.48	.44	241.45	1.4528	.6783	.8364	.8553	2.0590	.4	.259	.659	.55	-53.96
	2	5.36	10.05	0.	58.52	159.92	.181	65.43	1.834	.5591	3.06		1.911	1.273	0.	1.019	.55	105.60
29	1	4.29	11.40	0.	43.50	57.47	1.0	66.49	1.9724	.6944	.703		1.9400	.73	0.	.73	.69	117.89
	2	8.70	18.26	0.	-55.66	-50.11	1.0	113.31	1.8314	.5760	.693		1.9309	.52	0.	.92	.69	-110.80
31	1	12.36	23.43	0.	26.14	-8.49	1.0	354.39	1.7445	.1952	1.024		1.924	1.273	0.	1.015	.70	45.45
	2	13.61	20.22	4.80	93.98	-70.44	.376	115.05	1.6325	.5853	.9616	.6142	2.335	.675	.395	1.227	.70	120.83
32	1	4.56	9.117	3.63	-29.79	-48.42	.385	61.63	2.295	.5321	.8232		1.8785	.672	0.	.672	.80	-101.74
	2	7.16	20.09	17.44	12.69	25.57	.125	261.46	1.632	.6757	.8741	.6922	2.0597	.27	1.02	.397	.80	52.83
33	1	2.74	4.684	0.	-28.04	-138.0	.167	52.47	2.057	.6145	3.1513		1.630	.652	0.	.652	.60	-87.59
	2	3.128	14.62	13.57	3.91	13.09	.167	397.46	1.4747	.5495	1.125		2.055	.223	0.	.228	.60	25.29
37	1	15.79	23.96	0.	70.33	-14.73	1.0	200.16	1.6956	.2659	.8552		2.1987	1.444	0.	1.449	.60	82.3
	2	109.04	50.87	21.29	155.76	-100.82	.167	405.74	1.8491	.6160			2.332	.52	2.944	3.524	.60	85.15
39	1	14.14	13.35	5.62	184.58	26.83	.189	33.47	2.229	.7828	1.4531	.52116	1.995	1.254	.2	1.486	.53	274.2
	2	54.95	41.01	16.49	147.75	29.06	.189	357.84	1.113	.8324			2.183	.545	1.541	2.086	.53	78.60
41	1	27.35	31.26	8.85	-143.89	-194.99	0.	187.66	1.283	.6817			2.32	.622	.946	1.581	.80	-114.91
	2	11.75	24.31	0.	22.15	18.07	1.0	383.88	1.742	.1823	1.065		1.83	.652	0.	.686	.80	43.54
43	1	1.55	9.707	3.77	1.87	10.33	-1.0	697.38	1.182			.998	2.008	0.	.231	.231	.80	9.57
	2	1.96	7.108	0.	-20.54	-62.07	.385	58.07	1.930	.6190	1.525		1.70	.472	0.	.471	.80	-84.16
44	1	4.95	10.83	0.	68.27	44.03												

APPENDIX B

